

UC San Diego

UC San Diego Electronic Theses and Dissertations

Title

A Monolithic fabrication of pouch actuated soft robots

Permalink

<https://escholarship.org/uc/item/6k32m5xp>

Author

Zhang, Shuhang

Publication Date

2021

Supplemental Material

<https://escholarship.org/uc/item/6k32m5xp#supplemental>

Peer reviewed|Thesis/dissertation

UNIVERSITY OF CALIFORNIA SAN DIEGO

A Monolithic Fabrication of Pouch Actuated Soft Robots

A Thesis submitted in partial satisfaction of the
requirements for the degree Master of Science

in

Engineering Science (Mechanical Engineering)

by

Shuhang Zhang

Committee in charge:

Professor Nicholas Gravish, Chair
Professor Shengqiang Cai
Professor Michael Tolley

2021

Copyright
Shuhang Zhang, 2021
All rights reserved.

The Thesis of Shuhang Zhang is approved, and it is acceptable in quality and form for publication on microfilm and electronically.

University of California San Diego

2021

TABLE OF CONTENTS

	Thesis Approval Page	iii
	Table of Contents	iv
	List of Figures	vi
	List of Tables	ix
	Acknowledgements	x
	Abstract of the Thesis	xi
Chapter 1	Introduction	1
	1.1 Various fabrications of soft actuators	2
	1.1.1 Casting based fabrications	2
	1.1.2 Lamination and Origami fabrications	5
	1.1.3 Additive manufacturing fabrications	8
	1.1.4 Other fabrications	11
	1.2 Various actuation designs for soft robots	11
	1.2.1 Non-fluid actuation designs	12
	1.2.2 Fluid actuation designs	13
	1.3 Pouch actuators: Fabrications and Designs	15
	1.4 Summary	18
Chapter 2	Conceptual foundations	20
	2.1 Review of pouch motor principles	20
	2.2 Conceptual ideas of the monolithic fabrication	25
	2.2.1 Lamination	25
	2.2.2 Thermal bonding	25
	2.2.3 3d printing	26
	2.2.4 Design and modeling	26
	2.3 Choice of material system	26
	2.4 Summary	28

Chapter 3	Monolithic fabrication of pouch actuated mechanisms	30
	3.1 The filament welding method	30
	3.1.1 Modelling and parameters of the filament welding process	30
	3.1.2 Typical filament welding fabrication process	32
	3.2 The mask heat pressing method	34
	3.2.1 Overview of the mask heat pressing method	34
	3.2.2 Mask material choice via peel tests . . .	34
	3.2.3 Typical mask heat pressing process . . .	38
	3.3 Supplementary details	40
	3.3.1 Pouch geometry design	40
	3.3.2 Air inlets and connectives	41
	3.3.3 Equipment review	41
	3.3.4 Recommended parameters for 3d printing	42
	3.4 Summary	42
Chapter 4	Prototyping and Tests	44
	4.1 Single Pouch Actuator Tests	44
	4.1.1 Experiment setup	44
	4.1.2 Measurements and results	46
	4.2 Crawling robot demonstration	48
	4.2.1 Crawling robot design and fabrication . .	48
	4.2.2 Pneumatic control and driving system . .	48
	4.2.3 Movement demonstration	49
	4.3 Inherent motion sequence demonstration	51
	4.3.1 Viscous flow control theory for soft robots	51
	4.3.2 Fabrication of a sequential soft actuator	51
	4.3.3 Motion demonstration	52
	4.4 Summary	53
Chapter 5	Conclusion and Future Works	54
	5.1 Conclusion	54
	5.2 Conceptual extension and future works	55
	5.2.1 Embedded Sensors	55
	5.2.2 Improved mask heat pressing process . .	56
	5.2.3 Possibility of valves and logic	56
	5.2.4 One-station fabrication center	56
Bibliography	57

LIST OF FIGURES

Figure 1.1:	Soft lithography fabrication process for soft fluidic elastomer robots. Copyright Onal, C. D. & Rus, D.	2
Figure 1.2:	Fabrication of a bio-mimic fish body. Copyright Marchese, A. D. et al.	3
Figure 1.3:	An example scheme of lost wax casting which used a wax core during the molding process then melted it to form fluid chambers. Copyright Marchese, A. D. et al. . . .	3
Figure 1.4:	The SDM process proposed by Binnard, Mike and Cutkosky, Mark R.	4
Figure 1.5:	A rotational flexure mechanism and the corresponding fabrication flow. Copyright R.J. Wood et al.	6
Figure 1.6:	Laser machining part of SCM fabrication. Copyright Koh, Je-Sung and Cho, Kyu-Jin	6
Figure 1.7:	A lamination based fabrication to make soft hybrid bellows structures by Hee Doo Yang and Alan T. Asbeck .	7
Figure 1.8:	An exploded view(a), the actual prototype figure(b) and layer fabricated structure(c) of the "pneumagami" robot. Copyright Matthew A Robertson et al.	7
Figure 1.9:	Zhang, Yuan-Fang et al. multi-material 3d printing fabrication of soft actuator with incorporated shape memory polymers and tunable stiffness.	8
Figure 1.10:	States of fold based design soft actuator prototypes. Actuators were made by a single 3d printing process. . .	9
Figure 1.11:	Jiang, Mingsong et al. Schematic of the flexoskeleton method.	10
Figure 1.12:	Common approaches to actuation of soft robot bodies in resting and actuated states.	12
Figure 1.13:	Schematic of the manufacturing process of the robotic system with pouch motors by Niiyama, Ryuma et al. .	15
Figure 1.14:	The heat stamping system (top) and the heat drawing system (bottom). Picture by Niiyama, Ryuma et al. .	16
Figure 1.15:	A self-fold dodecahedron. (A) 2D design (B) automatically fabricated dodecahedron (C) dodecahedron self-folding process. Picture and captions by Xu Sun et al.	17
Figure 1.16:	A laser fabrication process for pouch actuators.	18

Figure 2.1:	Possible dimension changes and two actuation mode of pouch motors, Picture and captions by Niiyama, Ryuma et al.	21
Figure 2.2:	Prototypes of a linear pouch motor(left) and a rotational pouch motor(right). Picture and captions by Niiyama, Ryuma et al.	21
Figure 2.3:	Models of a single pouch. (a): a free pouch with cylindrical surfaces on both sides; (b):a pouch on a hinged joint. Picture and captions by Niiyama, Ryuma et al.	22
Figure 2.4:	Momentum-displacement-pressure plots of a typical hinged pouch motor model.	24
Figure 3.1:	Thermal analysis model of the filament welding process.	31
Figure 3.2:	Qualitative curve of temperature during the filament welding process.	31
Figure 3.3:	General filament welding process.	32
Figure 3.4:	Schematic of the filament welding process with support layer over pouch motors.	33
Figure 3.5:	Peel tests setup.	35
Figure 3.6:	Test samples schematic (a) and selected peel force measurement curves (b)-(e).	37
Figure 3.7:	Mask heat pressing fabrication process.	39
Figure 3.8:	Different layer arrangements for the mask heat pressing process.	40
Figure 3.9:	Motion sequence of a dual serial pouch actuator made by the mask heat pressing process.	40
Figure 4.1:	Design and fabrication details of the pouch motor samples for block force and bending angle tests.	45
Figure 4.2:	The test platform used for the bending angle and block force measurements.	45
Figure 4.3:	Electrical schematic of the test platform.	46
Figure 4.4:	Examples of block force measurement(a) and bending angle measurement(b) of the pouch motor test sample with size $25mm \times 25mm$	47
Figure 4.5:	Bending angle and block force test results of the 4 pouch motor samples with different geometries.	47
Figure 4.6:	Schematic of the filament welding fabrication of the crawling robot.	48

Figure 4.7: Electrical schematic of the crawling robot control system.	49
Figure 4.8: Motion sequence of the crawling robot. (hung in the air)	50
Figure 4.9: Motion sequence of the crawling robot moving on a wood surface.	50
Figure 4.10: Schematic of the fabrication of a self-sequence actuator.	52
Figure 4.11: Motion sequence of the self-sequence actuator	52

LIST OF TABLES

Table 2.1: Results from the thermal bond experiment	27
Table 2.2: Selected filament material properties	28
Table 2.3: Selected Sheet material properties	28
Table 3.1: Mask material peel force test results. Sample made by heat pressing at 260°F, 30 seconds, about $100N/cm^2$ pressure, tested at peel angle 180° and speed 60 <i>mm/min</i>	36
Table 3.2: Supplementary peel force results. Samples made by heat press at 260°F, 30 seconds, about $100N/cm^2$ pressure, tested at peel angle 180° and speed 100 <i>mm/min</i>	38
Table 3.3: Recommended 3d printing parameters for the monolithic fabrication. δ refers to the thickness of the heat pressed multi-layer base.	42

ACKNOWLEDGEMENTS

I would like to thank all the committee members of this thesis for supporting me in pursuing this degree, especially my director, Nicholas Gravish. His persistent encouragement and guidance have made this work a reality. His motivation and enthusiasm provided me with the motivation to move forward.

Thanks also to the members of the Gravish lab and other MAE department affiliates for all the help and support, especially during the crisis and uncertainty of the past year. My staying at UC San Diego has been an important chapter for me, no matter what my life may hold in the future.

ABSTRACT OF THE THESIS

A Monolithic Fabrication of Pouch Actuated Soft Robots

by

Shuhang Zhang

Master of Science in Engineering Science (Mechanical Engineering)

University of California San Diego, 2021

Professor Nicholas Gravish, Chair

In this work, a novel, monolithic fabrication method is proposed and developed. The proposed process aims at the fabrication of low profile, pneumatic soft robots driven by pouch actuators and combines the concepts of lamination, 3d printing and thermal bonding. Two different fabrication approaches, the filament welding fabrication and the mask heat pressing fabrication were introduced and tested, preferred manufacturing parameters were obtained by experiments. The fabrication, due to its simplicity and flexibility, enables prototyping of soft actuators with different applications and properties and therefore has the potential for future implementations in soft robotics.

Key words: Soft robots, Fabrication, Pouch motors, 3d printing, Pneumatic actuation.

Chapter 1

Introduction

The past two decades has witnessed an increasing amount of studies on soft robotics. By utilizing various compliant materials, soft robots are gifted with special features compared to their traditional, rigid counterparts, such as improved robustness, continuum deformation, safety for human interaction and better biocompatibility[1][2] while many of the soft robot designs were actually inspired by living organisms. The development of various novel fabrication techniques, notably, played a vital role in bringing about the advancement in soft robotics research as they enabled the creation of soft structures together with the embedded actuation, control and sensing[3][4][5]. This paper, however, would mainly focus on the fabrication of actuation structures.

Based on different actuation methods of soft robots such as fluid (gas or liquid), tension cables, Dielectric material or shape memory alloys, the fabrication techniques also vary from general molding and casting of elastomer materials[6], laminating and embedding process[7], Shape Deposition Manufacturing (SDM)[8] to multi-material 3D printing[9], soft lithography[10] and so on. These fabrication methods are often

combined with each other in practical design and manufacture of soft robot systems. In this chapter, a selected set from the library of soft-oriented fabrications will be generally reviewed together with some corresponding application in robot actuation and prototyping. Then, a novel, lamination and fused composition based fabrication will be introduced as a fast, simple and cheap approach to produce pneumatic actuated soft mechanisms.

1.1 Various fabrications of soft actuators

1.1.1 Casting based fabrications

Molding and casting of soft, compliant material such as rubber or silicon elastomer has been a popular and stereotypical method to make soft robots. Fluidic elastomer actuators (FEAs), specifically, are widely used in soft robot designs due to its adaptive, extensible and low-power properties. Fig.1.1 shows a lamination and casting based, soft lithography fabrication[11] for FEAs back to 2012; A similar progress is used for the fabrication of a bio-mimic soft actuator[12] as in Fig.1.2.

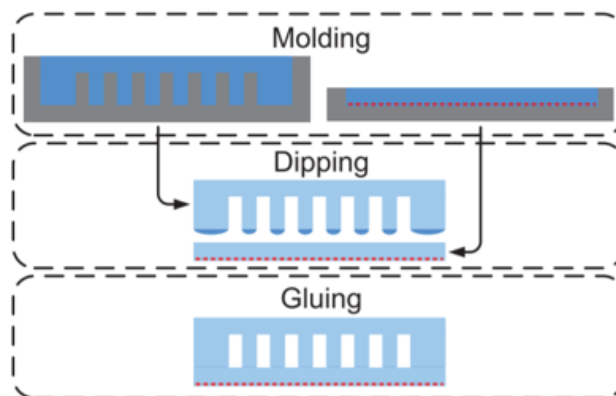


Figure 1.1: Soft lithography fabrication process for soft fluidic elastomer robots. Copyright Onal, C. D. & Rus, D.

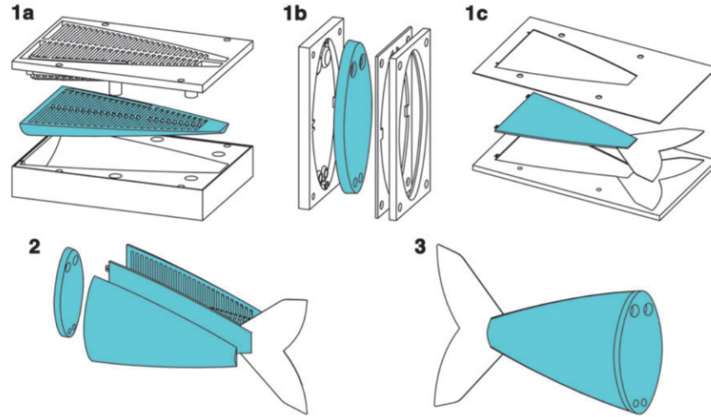


Figure 1.2: Fabrication of a bio-mimic fish body. The two halves of the body (1a), a connector piece (1b), and a constraining layer (1c) are cast separately then bonded as a whole piece. Copyright Marchese, A. D. et al.

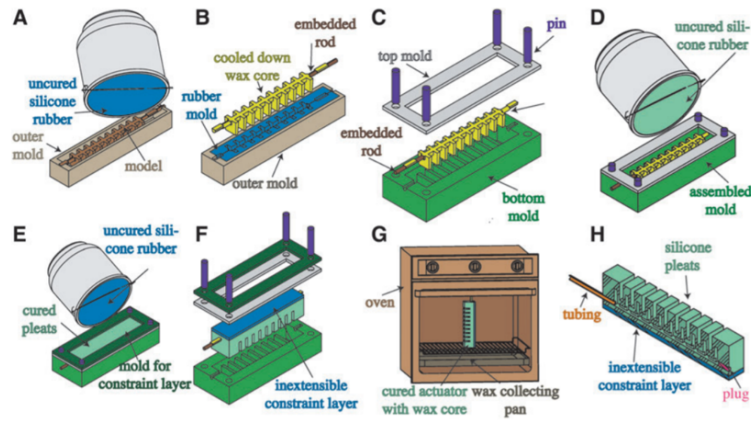


Figure 1.3: An example scheme of lost wax casting which used a wax core during the molding process then melted it to form fluid chambers. Copyright Marchese, A. D. et al.

Fig.1.3 shows a more developed fabrication approach[6][13] which eliminates the lamination process by using an internal wax mold then remove it by melting so that prevents potential issues of seams and delamination. In some related studies, other

soluble or flexible materials were also used to make the core components[14][15]. Other approaches to build up internal volumes and chambers within a monolithic cast of soft elastomer actuator includes directly extracting of the core[16] and rotational molding[17] when the internal structure geometries are not as complex and important.

Shape Deposition Manufacturing (SDM)[18][19], or more generally, embedded molding, is a more complex but integrated casting based fabrication for either rigid, metallic or soft structures. This method allows systematical embedding of electrical sensors, wires and other rigid components into a body of compliant and flexible materials by using a hybrid process of machining and molding. SDM was first applied for manufacturing robot parts around 2000 by Binnard, Mike and Cutkosky, Mark R.[20].

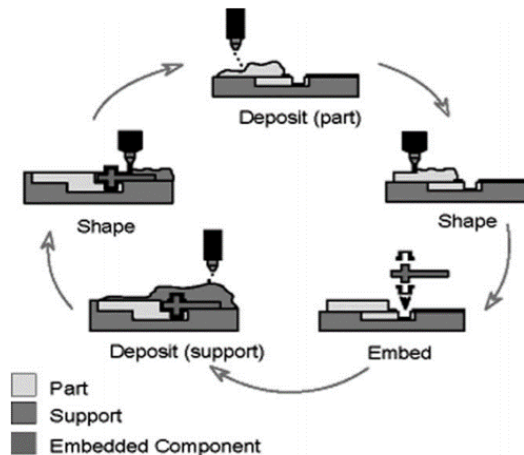


Figure 1.4: The SDM process proposed by Binnard, Mike and Cutkosky, Mark R.

Two representative application of this integrated fabrication in soft robotics are a hexapedal robot[8] powered by soft limbs in 2002 and a compliant grasper[21] which was composited of heterogeneous materials developed in 2006. Although with the

recent flourish of additive manufacturing methods and the prevalence of commercial grade 3d printers, SDM did not become a really popular research concept itself, the manufacturing ideas and methodologies contained in it, to some extent, are inherited and embodied by various embedded casting and deposition based fabrications pretty well, such as embedded sensors[22][23] or fiber reinforcements and strain limiting layers[24][25].

1.1.2 Lamination and Origami fabrications

The lamination based, thin-film fabrications which were adapted from microelectronics industry, have also become popular in the field of soft robotics. To fabricate rotating joints under a confined size limitation, some flexible film materials are used to form semi-soft hybrid, low profile mechanisms, which is known as the fabrication concept termed Smart Composite Microstructures (SCM)[7] proposed back to 2008 by R.J. Wood et al.

SCM specifically makes a integrated, planar structure with fiber reinforced rigid links and polymer flexure joints by combining laser-machining and lamination process, Fig.1.5 shows a scheme of the original SCM morphology while Fig.1.6 provides more details of the laser-machining part of the SCM process by Koh, Je-Sung and Cho, Kyu-Jin[26], who embedded SMA actuation with the SCM fabrication in their work.

Since lamination based fabrications are simple and suitable for making soft hybrid composite structures, they have also been adapted to soft robots in larger scales. Origami or folded robots, which has become an increasingly hot topic in the past few years[27][28][29], could also be interpreted to be a direct extension of the lamination fabrications because they also use composite fabric materials in very thin profile to achieve mechanical applications.

Some examples of recent developments in this field includes a couple of fabrication

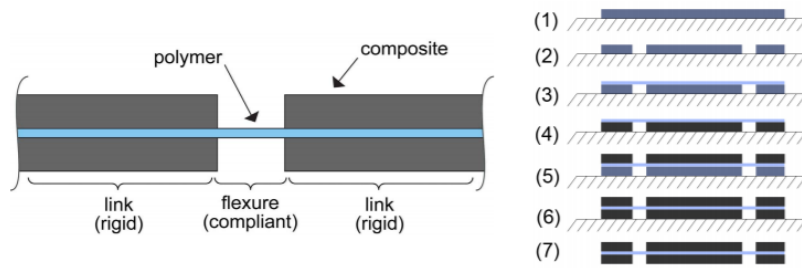


Figure 1.5: A rotational flexure mechanism and the corresponding fabrication flow. Copyright R.J. Wood et al.

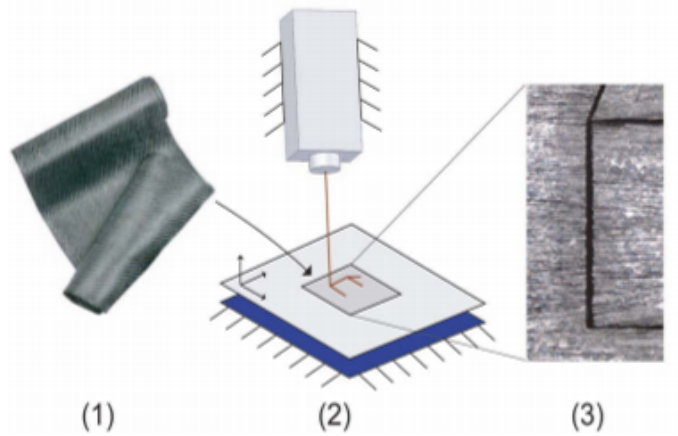


Figure 1.6: Laser machining part of SCM fabrication. Copyright Koh, Je-Sung and Cho, Kyu-Jin

designs[30] for making bellow-like actuators introduced by Hee Doo Yang & Alan T. Asbeck in 2018 and a novel pneumatic robot[31] developed by Matthew A Robertson et al in 2021. The illustration of corresponding fabrication details are shown in Fig.1.7 and Fig.1.8.

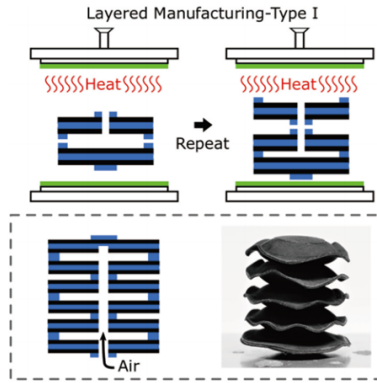


Figure 1.7: A lamination based fabrication to make soft hybrid bellow structures by Hee Doo Yang and Alan T. Asbeck

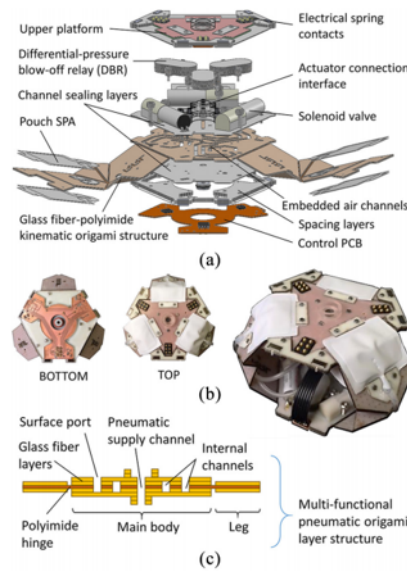


Figure 1.8: An exploded view(a), the actual prototype figure(b) and layer fabricated structure(c) of the "pneumagami" robot. Copyright Matthew A Robertson et al.

1.1.3 Additive manufacturing fabrications

With the prevalence of digital additive manufacturing methods, or more frankly speaking, various 3d printing techniques, a new family of soft robot oriented fabrications have been developed correspondingly[32]. Because of Fused Deposit Manufacturing 3d printing platforms, researchers are now able to prototype really fast using feasible polymer plastic materials, including PLA, ABS and especially the flexible, 3d printable materials like TPU. Many of them just used 3d printing for rapid tooling, such as making molds for elastomer casting in an accelerated way[33][24], which has become a widespread technique in soft robotics; In this part, some more direct applications of additive manufacturing will be discussed instead.

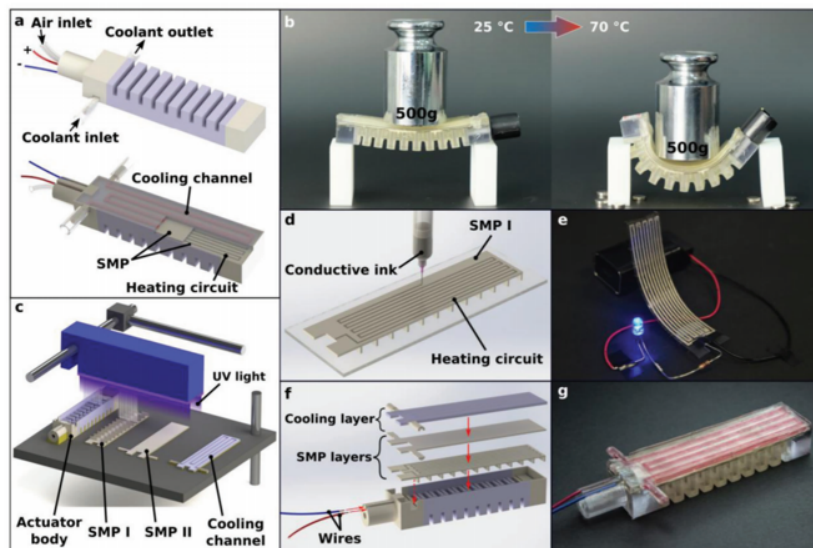


Figure 1.9: Zhang, Yuan-Fang et al. multi-material 3d printing fabrication of soft actuator with incorporated shape memory polymers and tunable stiffness.

Fig.1.9 is a scheme of a multi-material 3d printing fabrication[34] proposed by Zhang, Yuan-Fang et al. in 2019. In this work, they embedded heating circuits and shape memory materials into a typical pneumatic actuator body to achieve specified

properties; Common efforts have also been made in the direction of more integrated or monolithic fabrication, such as the 3d printed pneumatic soft actuator with embedded air connectors[35] by Stano, Gianni et al., the fold based soft actuator designs[36] using flexible material 3d printing by Keong, Benjamin et al. Some representative results of the latter work is highlighted in Fig.1.10.

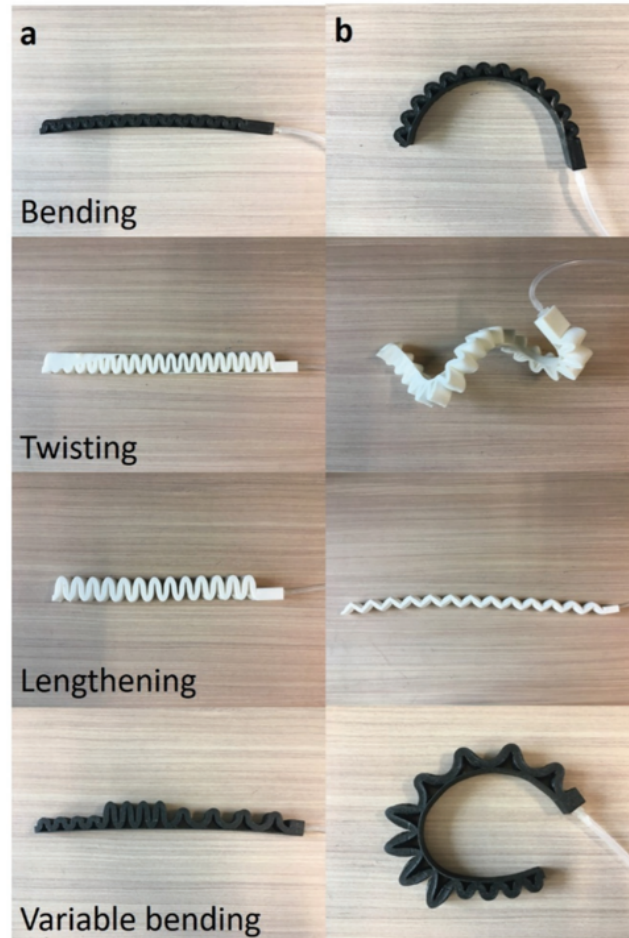


Figure 1.10: Keong, Benjamin et al. (a) Original state and (b) pressurized state of different fold based design soft actuator prototypes. Actuators were made by a single 3d printing process.

In 2020, Jiang, Mingsong et al. proposed a novel 3d printing approach[37] for making soft-rigid hybrid robots termed "flexoskeleton". Instead of printing the thermal plastic flexible materials, they printed rigid material like PLA or ABS onto a flexible polymer base sheet so as created hybrid structures of rigidity and flexibility. This fabrication is somewhat limited in dimension since it could be interpreted as a 2.5D process, but it's relatively faster and more robust compared to those used soft materials. Actuation, however, is not included in the fabrication, additional tension cables were used to drive the fabricated robot components.

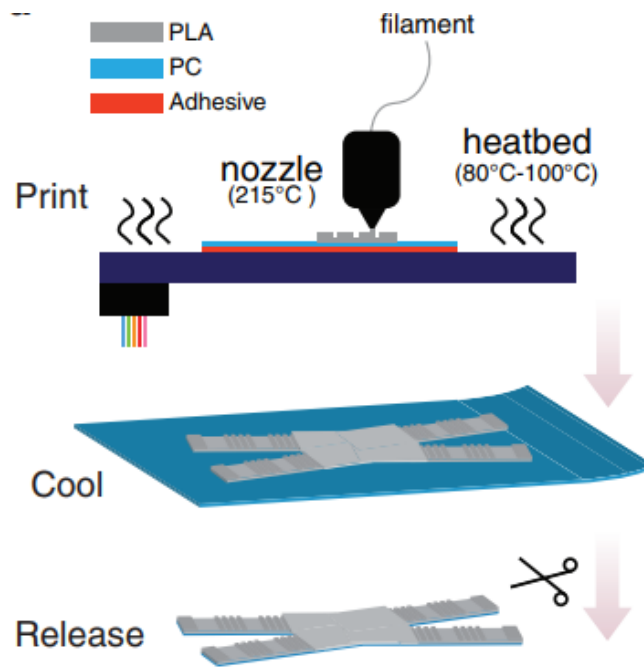


Figure 1.11: Jiang, Mingsong et al. Schematic of the proposed flexoskeleton method. 3d printing materials were thermally deposited and bonded to the plastic base to form a hybrid composite structure.

1.1.4 Other fabrications

Some fabrications for soft or semi-soft robotic systems can not be easily categorized into any general class of techniques. They either combine a number of different manufacturing methods, use commercial soft components directly or involve much manual labours within the process, such as the fabrication for various artificial muscles[38][39][40] from fabric, elastomer films, tubes and strings or electroactive smart materials. Other interesting fabrications include a quite unique method proposed by Nemiroski, Alex et al. in 2017, which used thin polymeric tubes and inflatable tubes to make bio-inspired arthropod-like-robots[41].

1.2 Various actuation designs for soft robots

Soft robots could be categorized by different actuation methods. Generally, they either use embedded variable length tendons such as tension cables and shape memory alloys for actuation, or use some fluid or pneumatic actuation to cause inflation and desired deformation in soft materials. Admittedly, many soft robot systems still rely on electric-mechanical components such as motors or air compressors as the source of mechanical power, this section will accept that but focus on the final transmission step.

Although fabrication and actuation are two aspects connected quite closely, there is no definite corresponding relationship between one type of fabrication with one type of actuation of soft robots. In this section, some commonly used soft actuation designs will be generally reviewed while one type of actuators termed as pouch actuators or pouch motors will be specifically elaborated to emphasize the inspiration of this work.

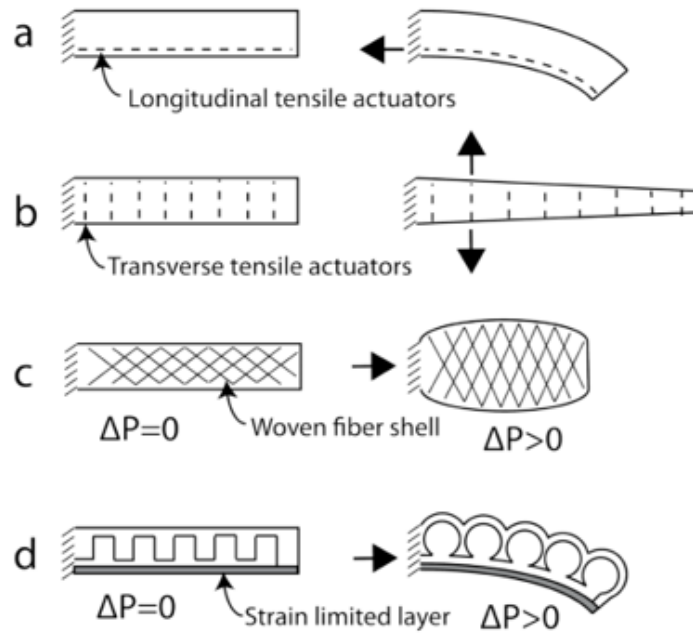


Figure 1.12: Common approaches to actuation of soft robot bodies in resting (left) and actuated (right) states. (a): Longitudinal tensile actuators; (b): Transverse tensile actuators cause a soft robot arm to extend when contracted. (c): Pneumatic artificial muscles composed of an elastomeric tube in a woven fiber shell; (d): Fluidic elastic actuator design that expands when pressurized and bends toward a strain limited layer. Figure and captions by Rus, Daniela & Tolley, Michael T., 2015.

1.2.1 Non-fluid actuation designs

Tension cable actuation

Cable driving has been a common actuation approach for both hyper-redundant, rigid link robots and soft robots. One classic application of this actuation is the "Elephant's Trunk" robot[42] proposed back to 1999, which was actuated by series of tendons routed through a rigid link structure. The robot has 32 degrees of freedom which enabled it to bend into numerous different shapes; Recently in 2017, Tang, Lei et al. proposed an alter version of cable-driven hyper-redundant serial robot[43],

which is able to perform quite accurate motions.

Similar actuation designs have been applied to soft robot systems as well, such as the octopus-inspired soft robot[44] proposed by Calisti, M et al in 2011. Follow up research includes a medical-purposed soft manipulator[45] and a mathematical analyse of the dynamic behaviors of a multi-bending soft robot arm[46] driven by cables. In 2020, Zappetti, D. utilized cable actuation in a novel tensegrity, semi-soft spine system[47], whose rigidity is controllable by the cables.

Smart materials actuation

Shape memory materials, which include shape memory alloys (SMAs)[48] and Shape memory polymers (SMPs)[49] are commonly used in soft robotics. This class of materials could change their shapes plastically but restore their initial shapes after a thermal stimulus; Electroactive polymers(EAPs) have also been explored as actuation materials due to their unique physical properties. Dielectric elastomer actuators (DEAs)[50] and ionic polymer metal composites (IPMCs)[51] are both under this general actuator class.

Magneto- and Electro-Rheological Materials are elastomer or fluid materials embedded with magnetic or electrical particles. This kind of material would react to external fields so as to cause a desired motion or deformation in a soft robot system[52][53]; Gels and hydrogel materials, which would react to optical, humidity or electro-chemical stimulus, have also been used for sensing or actuation for soft robots[54][55].

1.2.2 Fluid actuation designs

Pneumatic artificial muscles

Pneumatic artificial muscles (PAMs), sometimes termed as McKibben actuators, are compliant linear soft actuators composed of elastomer tubes in fiber sleeves

(PAMs)[56][57] which was first introduced back to the 1960s. Until recently, there have been continuous progress and new techniques on this topic such as the large stroke PAM[58] proposed by Cho, Hyun Sung et al. which utilized some bio-inspired rigid mechanisms, and the foldable fiber PAM design[59] by Naclerio, N. D. et al.

Fluidic elastomer actuators

Fluidic elastomer actuators (FEAs) or sometimes termed as Flexible fluidic actuators (FFAs), is an actuation technology which is especially common in soft robotics[60][61] because of low-cost elastomer materials, fast response time, and relatively higher actuation forces compared to some smart material approaches. As mentioned in the previous section, they are either molded and cast from various compliant silicon elastomer, polymer and rubber materials or manufactured by some integrated lamination and 3d printing process.

The actuation principle of FEAs is to utilize the expansion of embedded channels under pressure. Once actuated, an FEA would be able to hold the pressure and keep its position with out much power input. A strain limiting layer or component is often crucial to the mechanism of a FEA to create the asymmetric, bending motions. FEAs can be powered pneumatically, related designs could be tracked back to as early as 1990s[62]; The applications of pneumatic FEAs in recent years include the well-known multi-gait walking robot[63], the resilient, untethered robot[64] which is capable of working under hazardous conditions, and a rapidly-actuated network design[24] for pneumatic FEAs; In some studies, FEAs are actuated hydraulically, such as the underwater soft robot[65] by Katzschmann, R et al. and the soft robotic gloves[66] by P. Polygerinos et al.

Pouch Motors

In addition to the actuation methods above, there is a class of fluid actuators called pouch actuators, which have been drawing attention in recently. Some fabri-

cation methods and related actuator designs of pouch motors would be reviewed in the next section.

1.3 Pouch actuators: Fabrications and Designs

Pouch motors were first proposed by Niiyama, Ryuma et al. in a couple of consecutive works[67][68][69] around 2015. In their first paper, the group introduced a novel approach to use simple, inflatable pouches made from film materials as the actuators for folded mechanisms. Two different models, linear pouch motors and angular pouch motors were discovered and analysed. The motors were fabricated by heat bonding with mechanical pressure, and then attached to folded mechanical skeletons so as to create functional robotic components powered by compressed air, see Fig.1.13.

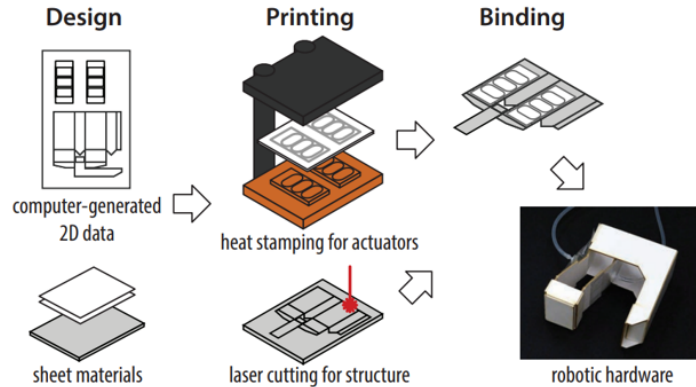


Figure 1.13: Schematic of the manufacturing process of the robotic system with pouch motors by Niiyama, Ryuma et al.

These pouch actuators, apparently, are suitable to be integrated into some layered, laminated rapid fabrication of printable or origami robots, because they themselves are in low profiles and made from a dual layer lamination process. In their

latter works, the group further developed the fabrication so that they were able to use both a heat stamping system and a heat drawing system to make the pouch motors (see Fig.1.14), they also made some prototypes of foldable origami robots such as the one in Fig.1.15. However, the pouches and the skeleton still need to be manufactured separately and bond with adhesive.

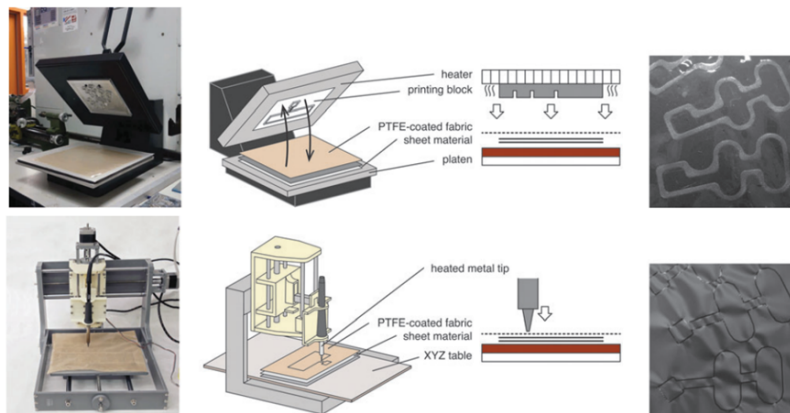


Figure 1.14: The heat stamping system (top) and the heat drawing system (bottom). Picture by Niiyama, Ryuma et al.

In 2016, a follow-up work[70] was presented by Ou, Jifei et al. The group introduced "aeroMorph", a new design space of inflatable shape-change materials focused on interactive applications. A three-axis CNC machine was build up for both sealing the coated fabric materials and cutting the materials into desired shapes. The shape changing materials are actuated by external air pressure with their bending directions smartly controlled by the folding creases created right during the thermal sealing process; Later in 2019, "milliMorph"[71], which is basically a hydraulic extension of the previous work, was proposed by the same group, and a similar work on fluidic fabric muscle sheets[72] was presented in 2020.

In 2018, Moghadam, Amir et al. developed a method to make thin soft pneumatic actuators rapidly[73][74] by laser cutting. Fig.1.16 shows the fabrication of a serial

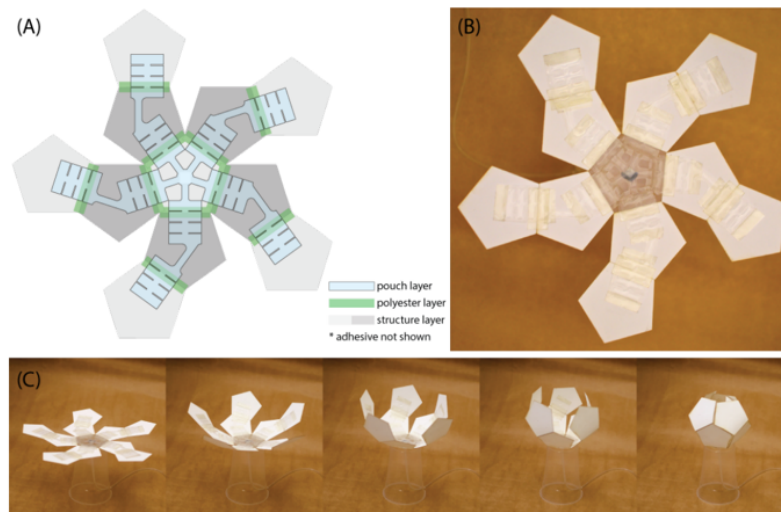


Figure 1.15: A self-fold dodecahedron. (A) 2D design (B) automatically fabricated dodecahedron (C) dodecahedron self-folding process. Picture and captions by Xu Sun et al.

bending pouch actuator. Two different type of actuators were designed to realize in- and out-of-plane bending motions; Bidirectional motion was achieved by stacking multiple bending actuators in a whole piece.

Some studies have also tried to integrate pouch-like pneumatic actuators with some complicated actuation systems. Around 2019, Christoph Keplinger¹'s group introduced a novel kind of hydraulically amplified self-healing electrostatic (HASEL) actuators[75][76], which adopted the shape and morphology of pouch motors but are actuated with hydraulic and electrostatic principles. The HASEL actuators were fabricated by both heat pressure stamping and CNC machine heat sealing, just like the previous works on pouch motors; Fatahillah, Mohammad et al. included pneumatic pouch actuation in the design of a novel soft bending actuator[77] powered by both positive and negative pressures; A novel flat fabric pneumatic artificial muscles[78] and a new design space of fabric bending actuators and inflatable robots[79] were

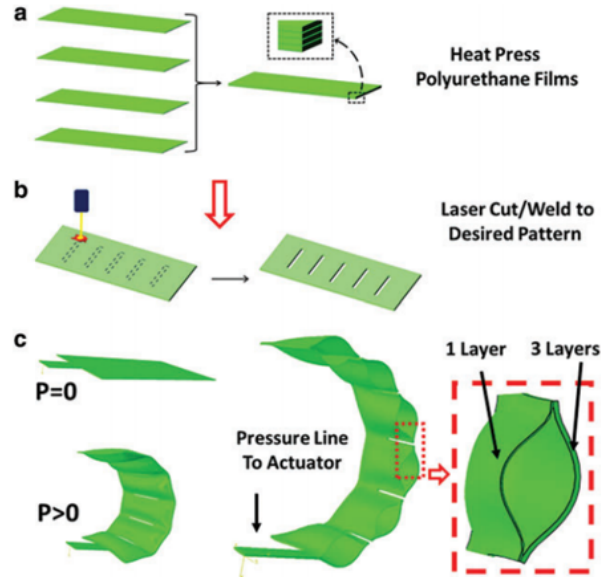


Figure 1.16: Laser fabrication process for pouch actuators. (a): Four layers of thermoplastic polyurethane are heat pressed to conformal contact. (b): A laser beam cuts the layers with a desired pattern. (c): The inflated chamber is bounded by one and three layers on its sides; the asymmetry of the stiffness leads to a bending motion. Picture and captions by Moghadam, Amir et al.

also based on pneumatic pouch motors.

1.4 Summary

Given all the previous actuation and manufacturing research mentioned above, especially those works about lamination-based fabrications and pouch motors, it is natural to think about if a more integrated and fast fabrication technique could be developed to explore a design space of soft pneumatic robot which could be designed and manufactured rapidly with low cost and minimum equipment or labour requirements so as to boost the application of soft robots to some extent.

In this work, a new monolithic fabrication method will be proposed and tested for pneumatic pouch actuated soft mechanisms. The new fabrication will combine lamination and additive manufacturing techniques and could be interpreted as a combination of flexoskeleton[37] with inherent pouch motor actuation. In the next chapter, some basic concepts, objectives and constrains of the proposed method will be identified and clarified; Then in chapter 3, the general methodology and technique details of the proposed monolithic fabrication will be presented; In chapter 4, some prototypes made through the fabrication are tested; In the final chapter, the results from this work will be reviewed and evaluated, together with some possible future research directions.

Chapter 2

Conceptual foundations

2.1 Review of pouch motor principles

This work focuses on the application of pneumatic pouch motors. Upon pressurized, these motors would inflate, deform into cylinder-like shapes and provide the power needed for actuation. The mathematics models and driving principles of pouch motors had already been analyzed and derived pretty well [68] by Niiyama, Ryuma et al. Pouch motors have two types of dimension change: Linear retraction and angular rotation, thus there are both linear and angular pouch motors (see Fig.2.1 and Fig.2.2).

To build the theoretical models of pouch motors, some assumptions and simplifications were adopted. A free, inflated pouch motor is assumed to have the shape of an airfoil, with the both top and bottom surfaces to be cylindrical; While for a pouch motor with hinge constraint, the shape would be slightly different.

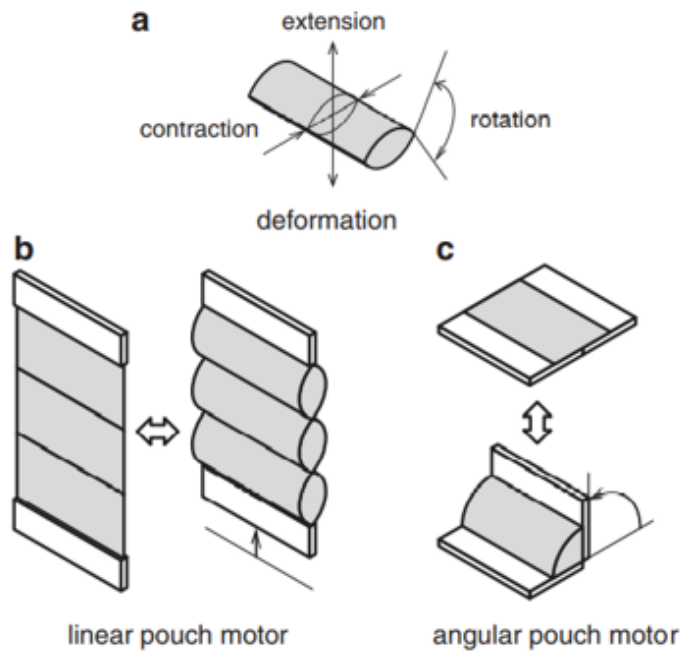


Figure 2.1: (a):Possible dimension changes of a pouch. (b):linear actuation mode; (c): Angular actuation mode. The gray and white parts indicate inflatable pouches and stiff structure, respectively. Picture and captions by Niiyama, Ryuma et al.

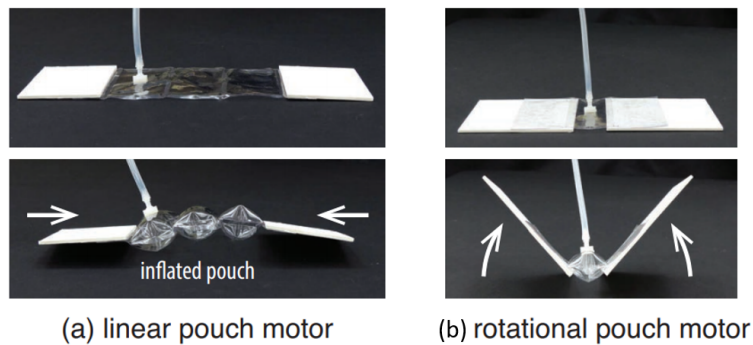


Figure 2.2: Prototypes of a linear pouch motor(left) and a rotational pouch motor(right). Picture and captions by Niiyama, Ryuma et al.

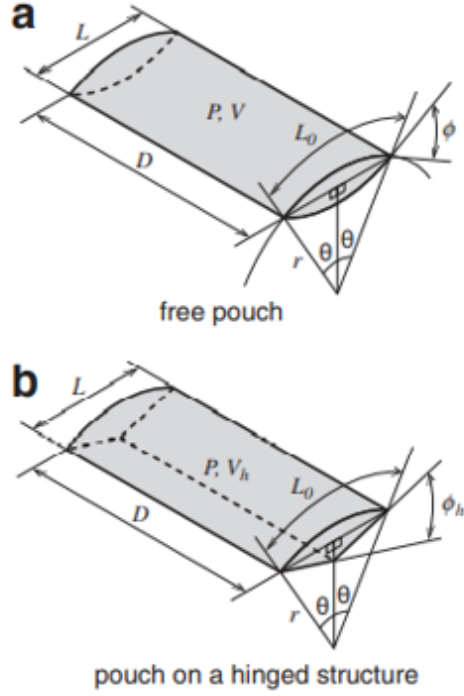


Figure 2.3: Models of a single pouch. (a): a free pouch with cylindrical surfaces on both sides; (b):a pouch on a hinged joint. Picture and captions by Niiyama, Ryuma et al.

Fig.2.3 shows the dimensions and symbols of both types of pouch motors. Side areas and elastic deformation are neglected for simplicity of derivation. Thus the volume of a pressurized, free pouch motor was derived as:

$$V(\theta) = \frac{L_0^2 D}{2} \left(\frac{\theta - \cos\theta \sin\theta}{\theta^2} \right) \quad (2.1)$$

and for a hinged pouch motor, the volume V_h has the format:

$$V_h(\theta) = L_0^2 D \frac{\theta - \cos\theta \sin\theta + \sin\theta \sqrt{\theta^2 - (\sin\theta)^2}}{4\theta^2} \quad (2.2)$$

Apply virtual work method to the volume equations, i.e., $-FdL = PdV$ for a linear actuator and $Md\phi = PdV$ for an angular actuator, where P is the applied pressure for actuation, F and M correspond to the output force and momentum so that:

$$F(\theta) = L_0 DP \frac{\cos\theta}{\theta} \quad (2.3)$$

$$M(\theta) = L_0^2 DP \frac{\cos\theta(\sin\theta - \theta\cos\theta)}{2\theta^3} \quad (2.4)$$

$$M_h(\theta) = \frac{L_0^2 DP}{8\theta^2} (-1 + \theta^2 + \cos 2\theta - \sqrt{2}\cos\theta\sqrt{-1 + 2\theta^2 + \cos 2\theta}) \quad (2.5)$$

where $F(\theta)$ is the output force of a linear actuator, $M(\theta)$ is the output momentum of a free angular actuator, $M_h(\theta)$ is the output momentum of a hinged angular actuator, all conditioned on the pneumatic pressure P and pouch deformation angle θ .

Given the too ideal assumptions, these theoretical results turned out to have some limits and singular points. For example, given any non-zero P , $F(\theta)$ would reach infinity as $\theta \rightarrow 0$; given $P = 0$, the deformation θ could be any value in its domain, and so is the volume $V(\theta)$. In reality, non of these singular results seemed to be possible.

To clarify the pouch motors behaviors further more, consider taking the hinged, angular pouch motor as an example, and assume there is an inevitable, linear elastic coefficient in the hinge so that $M(\theta) = k\phi$ under no external momentum load. With higher or lower k values, the relationship between pressure, angular displacement and pouch position (According to Equation 2.5) are briefly depicted in Fig.2.4, where the black curves represent momentum-theta functions of the pouch motor under different pressure value, and the red rays represent the momentum-theta functions of hinges with different elasticity.

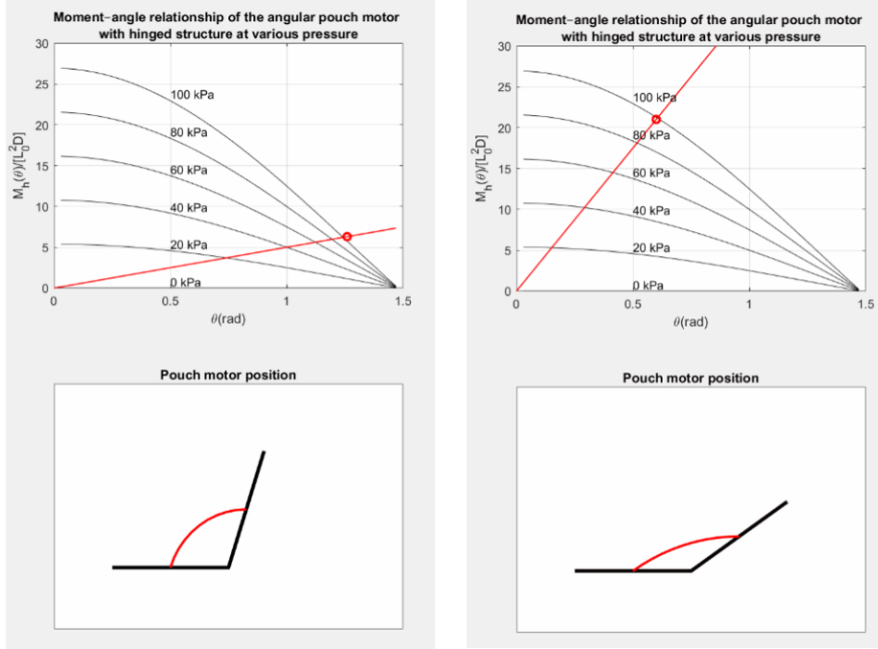


Figure 2.4: Momentum-displacement-pressure plots of a typical hinged pouch motor model with lower hinge resistance(left) and higher resistance(right). Pouch position plotted with 100 kPa (0.98 atm) pressure.

From the plots in Fig.2.4, it is clear that an over strong hinge or any constraint would put a limit to the motion space of a hinged pouch motor. To maximize the function of a fabricated pouch motor, the middle part of the hinge should be constructed with properly low strength while the other parts should remain rigid enough to transmit the output power.

Instead of a hinge joint, a continuum strain-limiting layer could also be adopted to support an angular pouch actuator; In this case, the model would become more complicated and combine the properties from both the free and the hinged pouch motors.

2.2 Conceptual ideas of the monolithic fabrication

In the past chapter, common fabrication methods of pouch motors were introduced. Thermally welded, heat pressed or laser cut, no matter how, the pouch motors usually needs to be attached to a supporting structure to fulfill its function and this process would always involve the use of adhesion material and extra labour. Given the low profile property of pouch motors and all the lamination-based fabrications of soft robots, it is an feasible association that some integrated fabrication could be developed.

2.2.1 Lamination

A pouch layer, which is made by some previous mentioned methods, could be inserted into a stacked composite of different material layers then provide actuation for the whole structure. Meanwhile , the geometry designs and lamination order of the laminated composites should allow the pouches to inflate and actuate without being interfered. Given such constraint, the angular pouch motors would be preferred to be used in lamination composites instead of the linear ones.

2.2.2 Thermal bonding

Common fabrication approaches for pouch motors involve utilizing heat to melt and seal plastic materials. From the previous literature review, it is clear that thermal bonding methods are used to fabricate some multi-layer structures, too. Combing the seal of pouches and the bond of multi-layer materials in a single or sequential thermal welding or heat pressing process is possible, such a technique would help to simplify and boost the fabrication.

2.2.3 3d printing

Fused deposit modeling (FDM), which is the most common 3d printing technique, involves heating, fusing and depositing of plastic filaments during its process. A 3d printer hot printer nozzle could very likely be used for thermal welding the contour of designed pouch motors.

The flexoskeleton[37] paper had found out that PC (polycarbonate) could bond with common 3d printing materials such as PLA(polylactic) and ABS(Acrylonitrile Butadiene Styrene) under their extrusion temperatures and thus create a semi-soft hybrid structure. However, after some primary experiments, PC is proved to be much too rigid and brittle to be used to make pneumatic pouches. If a suitable soft, thermalplastic material is found to be thermally bond with common 3d printing filament materials, then it's possible to make similar composite structures but with inherent actuation.

2.2.4 Design and modeling

The proposed fabrication would be largely constrained within a planar space due to its lamination based natural. The motion of inherent pouch motors would be limited in the out-of plane direction and the number of the whole structure's freedom degrees would be small. Proper model designing is needed to compensate such disadvantages.

2.3 Choice of material system

A suitable sheet material for making the pouch motors should meet the following criteria: First, thermoplastic and easy to seal; Second, be strong enough to hold the pneumatic pressure and survive the fabrication, but not too rigid to deform; Third, a similar melt point with common FDM 3d printing filament materials, would bond

with at least one common FDM filament; Finally, commercially available and affordable.

A thermal bonding experiment was completed to find a feasible material system for the fabrication. 3 types of common FDM materials were tested with some common film and sheet materials. A soldering iron was used to heat the materials to the melt point of the filament materials to simulate the FDM 3d printing process.

Table 2.1: Results from the thermal bond experiment

Filament materials	Sheet or film materials				
	PC	Nylon	PET	PE	TPU
PLA	True	False	False	False	True
ABS	True	False	False	False	True
TPU	True	False	False	False	True

Table 2.1 shows the results from the tests, a "True" result means there is a usable bond and a "False" result means no usable bond. Apparently, the tested 3d printing filament materials could all produce usable bond with TPU and PC sheet materials under the experiment condition. TPU (Thermoplastic polyurethane) is a class of soft, elastic material with unique properties and some different chemical formulas; The TPU film material used in this work is polyester-based and has a larger elastic modulus than the polyether-based type. Previous works such as [73] have already proved TPU's capability to form pouch motors.

PC is a rigid material with high Young's modulus. When formed as sheets, it is flexible but durable and could serve as the skeleton or strain limiting layer for a laminated structure, as previous mentioned in [37]. All these materials mentioned above are complex composite mixture of polymer materials and their properties vary by producers, some typical properties of the materials were collected in table 2.2.(Sources: Simplify3D[®], ©2021, 3DMaker Engineering, ©2021, All3DP); PC

and TPU are used as sheet materials in this work. Some potentially useful data are collected in table 2.3. (Sources: Prospector[®], McMaster-Carr[®], ©2021, MatWeb)

Table 2.2: Selected filament material properties

Properties	Filament materials		
	PLA	ABS	TPU based flexible
Extruder Temperature (°C)	190-220	220-250	225-245
Bed Temperature (°C)	45-60	95-100	45-60
Tensile Modulus (MPa)	2900-3500	1100-2900	12-396
Max Service Temperature (°C)	52	98	60-74
Durability	medium	high	high

Table 2.3: Selected Sheet material properties

Properties	Sheet materials	
	PC	Polyester-based TPU
Melting Temperature (°C)	140-232	106-227
Thickness (mm)	0.2, 0.3	0.2
Elasticity Modulus(Mpa)	1606-2675	140-730
Producer	McMaster-Carr [®]	David Angie [®]

2.4 Summary

In this section, the driving principles of pouch motors are explained and reviewed, the formulas related to output momentum are introduced in details which would be helpful to characterize and evaluate the yet to introduced pouch fabrication. General initial ideas, inspirations and methodology logic of the work have been further

explained. Next, primary thermal bonding experiments and material analysis were completed to build a feasible material system for the fabrication. With all those basic results acquired, in next section, the main part of this work, the new monolithic fabrication for pouch driven soft actuators will be discussed.

Chapter 3

Monolithic fabrication of pouch actuated mechanisms

3.1 The filament welding method

3.1.1 Modelling and parameters of the filament welding process

In this part, a method of sealing and making pouch motors by the hot nozzle of 3d printers will be introduced. Fig.3.1 shows the qualitative model of such a filament welding process, where δ is the thickness of the sheet materials, h is the Z axis offset of the 3d printer nozzle. Interface and extruded material effects were ignored for simplicity. The value of h should be almost identical but a little smaller than δ so as to create a heat conductive interface with area S_N . Sheet materials should cohere with the heat bed as flat as possible to produce an even and controllable weld result.

Consider a random interface point between 2 sheet materials (TPU in this case) along the trajectory of the hot nozzle. Denote heat bed temperature T_b , hot nozzle temperature T_h and the melt point temperature of sheet material T_m . With the

traveling of the hot nozzle, the temperature at the selected point $T(t)$ would rise to some value close to T_h and then decrease toward T_b , and if there is a time window Δt during which the temperature keeps above the melting threshold temperature T_m , that point would be thermal bonded after cool down. Fig.3.2 is an example schematic of the process, neither the values nor curve is based on real data.

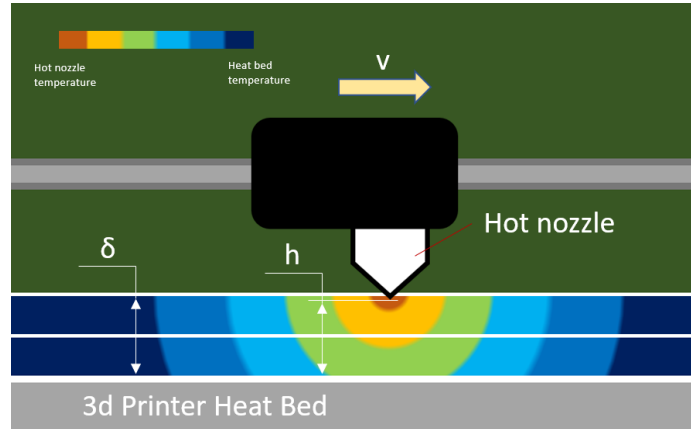


Figure 3.1: Thermal analysis model of the filament welding process.

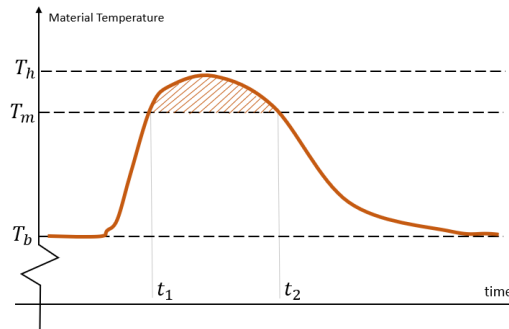


Figure 3.2: Qualitative curve of temperature during the filament welding process.

Apparently, the shadowed area in Fig.3.2 is crucial to the welding result. Assume

the strength of thermal welded bonds depends positively on the shadowed area, i.e., a partial integral of temperature along time and it would be a complex function involving T_b , T_h , T_m , δ , h , the traveling speed of hot nozzle v , and the thermal conductivity of TPU sheet material c_{TPU} . Here, T_h and T_b are considered to be less controllable parameters because they should always be set according to the filament material so as to ensure acceptable results of the 3d printing process; Whereas the Z offset h and travel speed v of hot nozzle are up to the choice of the user and should have a significant influence on the filament welding results.

3.1.2 Typical filament welding fabrication process

First step of the fabrication is to heat press a multi-layer base using a heat press machine. For the simplest case, 2 TPU sheets, a suitable heat press temperature should be around 210-220°F, with the pressure around $100N/cm^2$ and heat press time between 20 to 30 seconds, this would ensure a solid but not too strong bond between the TPU sheet materials. After the sealing process, the non-welded parts would still be easily separable to create the desired inflatable pouch chambers. see Fig.3.3. Note that the heat pressed sheet materials are secured to the heat bed with common glue sticks.

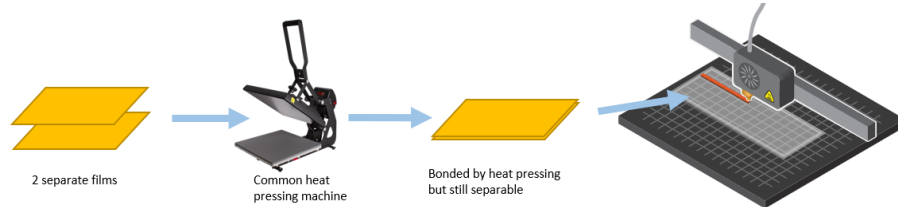


Figure 3.3: General filament welding process.

In addition to just making the pouch motors, a strain limiting and support layer should be integrated to the fabrication. As mentioned previously, the material of

this supporting layer chosen to be polycarbonate (PC). Depending on the position of this PC layer, the fabrication would be slightly different.

Support over pouches

In this case, an extra piece of PC is applied over the pouches. To make this happen, it is necessary to introduce a pause and manual operation step right after the pouch structures being finished by using pause & resume commands in the Gcodes generated from the 3D slicer software, for example:

```
G1 X10.000 Y10.000 E0;
```

```
M1;
```

```
M105;
```

The commands above would simply move the hot nozzle away from the working space and pause the 3d printing process. After finishing the necessary operations, the user would be able to push the control button on the 3d printer and finish the remaining part. Fig.3.4 shows the details of this fabrication process.

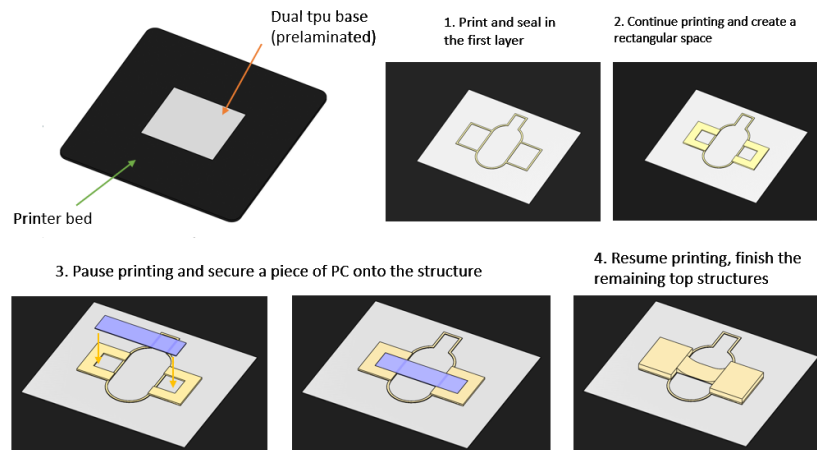


Figure 3.4: Schematic of the filament welding process with support layer over pouch motors.

Support under pouches

Sometimes the support might be expected to be on different side with the 3d printed structures. In this case, a PC layer could be heat pressed together with the dual TPU layers during the initial heat pressing process so that a 3 layers base sheet is used for the filament welding process. Extra thermal bonding strength is needed to bond the 3 layers firmly. The support layer could be either larger or smaller than the pouch layers, which is up to the design requirements. Positioning is required to secure the relative position between 3d printing and the support layer.

3.2 The mask heat pressing method

3.2.1 Overview of the mask heat pressing method

Many research groups use mold heat pressing to make pouch motors. This would ask for manufacturing of metal molds for every single design, which slows down the whole fabrication process and increases the cost. In this part, a similar process called mask heat pressing is introduced to overcome those disadvantages. By adding an extra layer of non-heat-bondable material between two TPU films then go through a very strong heat pressing process, a inflatable chamber with desired shape and size would be created immediately. Then the multi-layer base material is attached to the 3d printer heat bed so that extra functional structures could be added on. filament welding of pouches is not needed anymore.

3.2.2 Mask material choice via peel tests

An ideal mask material should not bond TPU films when heat pressed. This material could be some non-stick plastic with very high melt temperature and minimum physical affinity with polyurethane, preferably some ink or paint. If there is

such kind of ink, it is then possible to ink-print pneumatic chambers and channels to TPU films directly, then heat press them to create a complex pneumatic system.

Here, a set of peel force tests were completed to evaluate the strength of the bonds created by the heat pressing process. A couple of different mask materials were tested, Fig.3.5 demonstrates the method of peel tests. In this test, peel force results were measured at 180° , peel speed $60\text{mm}/\text{min}$.

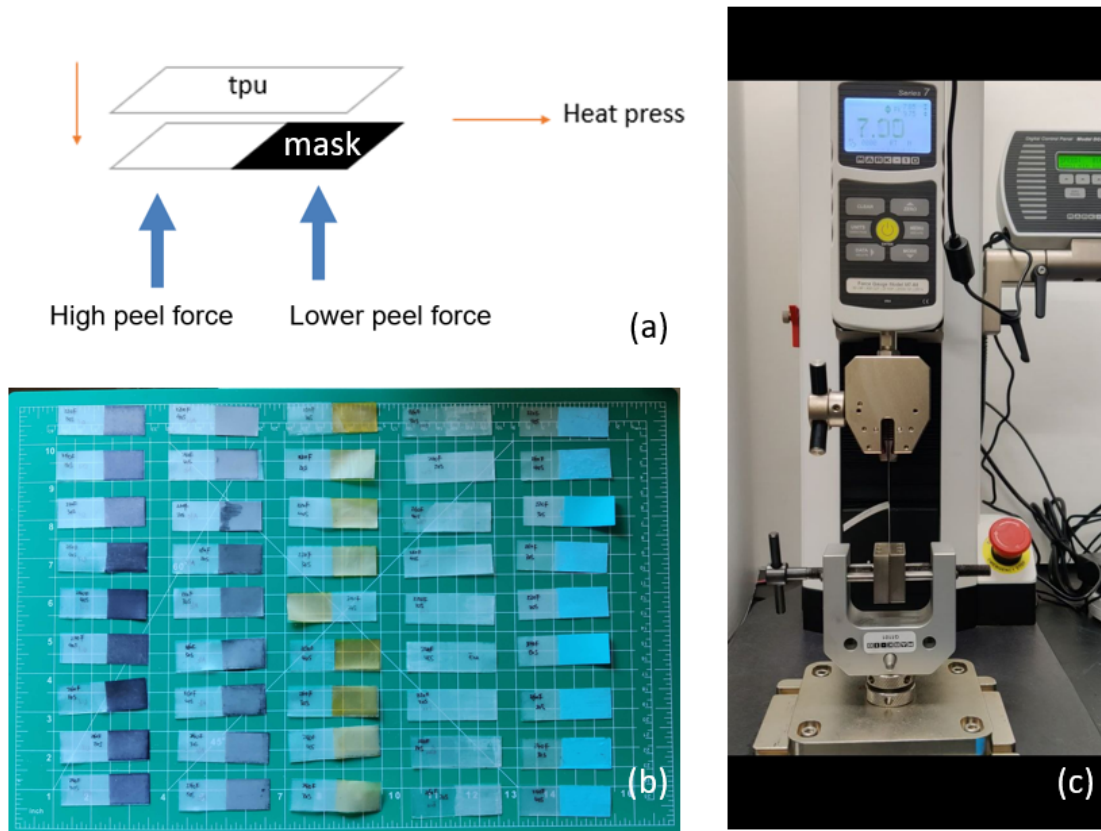


Figure 3.5: Peel tests setup. (a): Peel test samples sized $50\text{mm} \times 20\text{mm}$ (b): Photo of peel test samples with different mask material and heat press parameters. (c): Peel test equipment ESM750 measuring the peel force from a sample. (High-Capacity Motorized Test Stand).

The peel test begins with the mask area and then goes beyond, if these materials are able to reduce the peel force to some extent, the result measurements should begin with some low value and then drastically increase to some large value and keep steady. The curve should look like a sigmoid function.

However, with high heat press temperature over 260°F and enough heat press time, the bond of non-mask area is so strong such that the whole sample would be exaggeratedly elongated. In this case, it is not really possible to tell the accurate value of peel force, but it's sure large enough to make a pouch motor which can hold a significant amount of gas pressure. After processing and analysing the collected data, a representative result group is chosen to compare the performance of six selected mask materials, see table 3.1

Table 3.1: Mask material peel force test results. Sample made by heat pressing at 260°F, 30 seconds, about $100N/cm^2$ pressure, tested at peel angle 180° and speed 60 *mm/min*.

Mask material	Peel force (N/cm)	Simplicity to use
No mask (Control Group)	>10	-
Acrylic paint	0.166	Medium
Petroleum Enamel	0.334	Low
Oil-based permanent marker ink	0.152	High
Alcohol-based dry-erase marker ink	0.116	High
Kapton film	0.171	Low
FEP film	0 (No bond)	Low

Apparently, FEP film is an almost perfect material for heat press masks, but it needs to be cut into desired shapes. In this work, a laser cutting machine (glowforgeTM Glowforge basic) is used to make the FEP film material inserts, which increases the complexity and difficulty of the whole process.

On the other hand, if a paint material is used instead, then it is possible to use some ink printer or CNC drawing machine to print the pneumatic circuits directly on the TPU films. According to the results above, alcohol based dry-erase ink is the best choice of paint material so far. Kapton sheet molds were made by laser cutting to help applying the ink to TPU films to create patterns.

Another round of peel force tests is finished to better understand the behavior of alcohol based ink as mask material as well as the strength of thermal bond between heat pressed TPU films. This time, 4 different heat press time were tested while heat press time is set to be 30s unchanged. 5 samples were made under each temperature to minimize random errors.

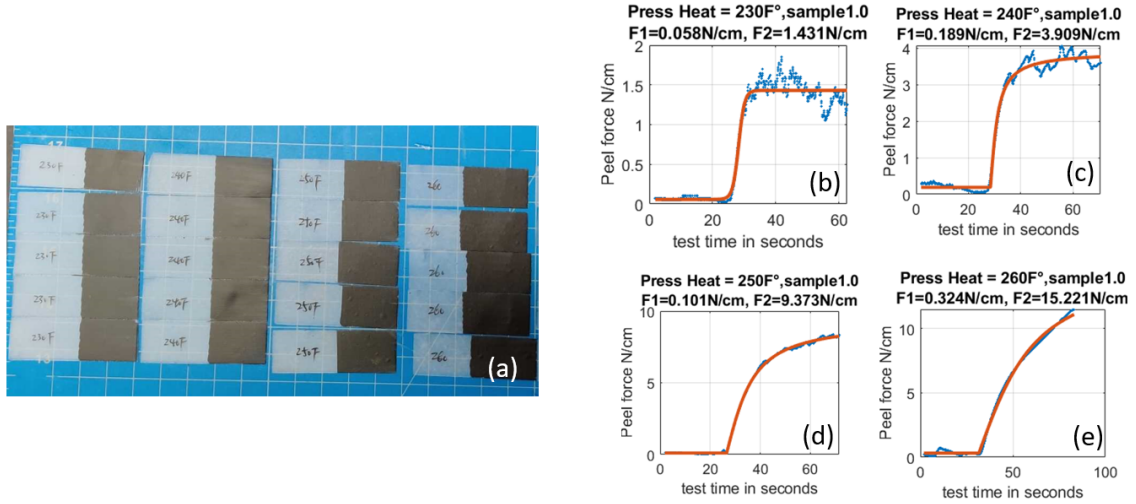


Figure 3.6: (a): Peel test samples sized 50mm \times 20mm. (b)-(e): Selected measurements of peel force curve with respect to test time under different temperatures. Heat press time 30s, peel speed 100 mm/min , peel angle 180°.

Fig.3.6 demonstrates the details of the second round of peel tests. Only Alcohol based dry erase marker ink was used to make the samples. A simple linear regression method was used to fit the data points (blue) with sigmoid functions or half-sigmoid

functions, which are plotted as orange curves in the plots, the peel force measurements were determined by the fit result functions parameters (F_1 and F_2 correspond to the mask peel force and non-mask peel force respectively).

By taking the mean values of measurements from all 5 samples, typical reference values of peel force were derived. Meanwhile, a similar test group with heat pressed PC and TPU (no mask) samples had been finished under exactly the same heat press parameters and sample setup. Table 3.2 summaries supplementary peel force data of the tested materials.

Table 3.2: Supplementary peel force results. Samples made by heat press at 260°F, 30 seconds, about $100N/cm^2$ pressure, tested at peel angle 180° and speed 100 *mm/min*.

Peel force (N/cm)	Temperature (°F)			
	230	240	250	260
Sample types				
2 TPU films	2.153	4.375	8.410	>10
2 TPU films with ink mask	0.041	0.100	0.133	0.307
TPU and PC films	0.514	1.031	2.760	4.829

3.2.3 Typical mask heat pressing process

From the peel tests above, it is clear that if a high heat press temperature over 260°F is applied, the non-masked area of two TPU films would be bonded firmly while the masked area (with suitable mask material) would be still separable.

FEP and alcohol based, dry erase marker ink are selected to be two mask materials in this work. For a film material like FEP, the first step is to cut it into desired shape of pouches and channels. Designing is finished by CAD software then sent to the laser cutting machine. Then, the mask is inserted into 2 TPU films and then heat pressed firmly, this would create a inflatable chamber inside the heat pressed multi-

layer structure. This method requires cautious manual operation since the laser cut masks can be quite thin, soft and fragile. The plastic film masks can be distorted during the process and cause deviations from the original design.

The other approach, is to use a paint material like the dry eraser marker ink. It is then possible to develop a print system or 2 axis drawing machine to plot desired pneumatic shapes on TPU films. Notably, the dry erase marker ink can not completely prevent thermal bonding between two films, so a better ink or paint material is still yet to be found. In this work, laser cut molds are used as a temporary method to apply ink masks. Details of the two different mask processes is demonstrated in schematic Fig.3.7.

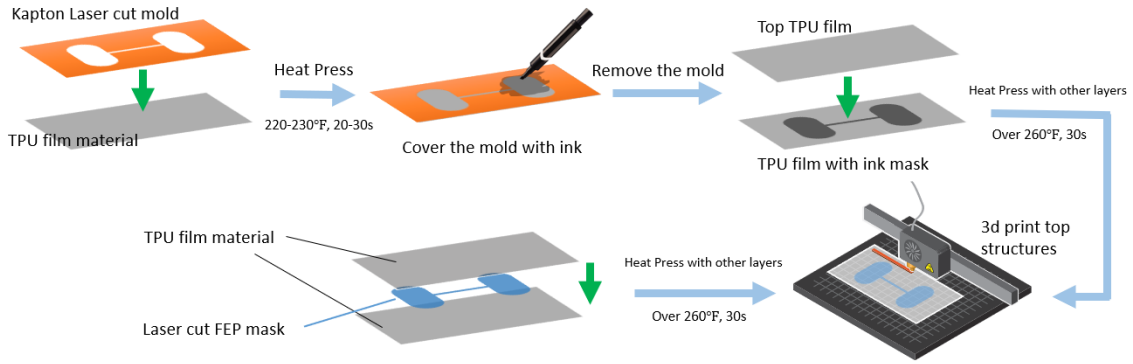


Figure 3.7: Mask heat pressing fabrication process. Top row: Mask made from ink material; Bottom row: Mask made from FEP film material.

PC is still used as support layer material in this fabrication and should be heat pressed with TPU and mask material. Especially, with 1 PC layer in the middle and 2 mask pouch layer groups by its both sides, it is possible to create a bidirectional actuator through a single heat pressing process, see Fig.3.8 for some examples of different layer arrangements and Fig.3.9 for the demonstration of an actuator fabricated by the mask heat pressing method.

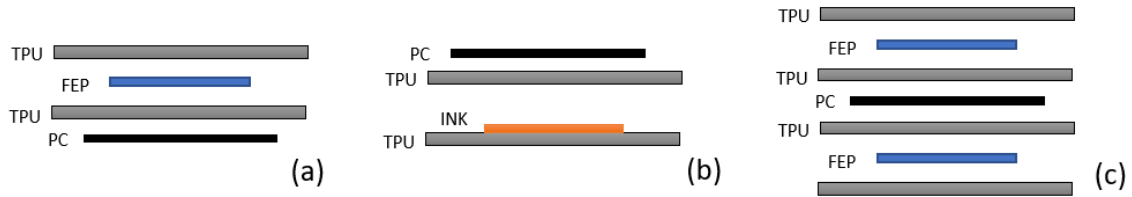


Figure 3.8: Different layer arrangements for the mask heat pressing process.(a): support under single pouch layer group, FEP insert mask; (b): support over single pouch layer group, ink mask; (c): support between two pouch layer groups, FEP insert mask.

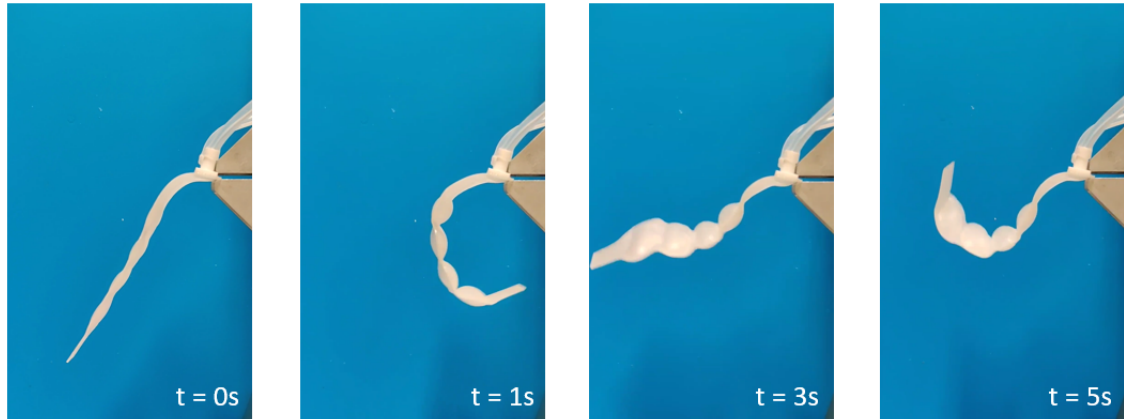


Figure 3.9: Motion sequence of a dual serial pouch actuator made by the mask heat pressing process. The actuator is powered by 2 independent pneumatic syringes. 3d printing process was not used to make this prototype, the actuator is thus too soft to hold itself.

3.3 Supplementary details

3.3.1 Pouch geometry design

Pouch motors were generally in rectangular shapes. The linear edges of the rectangular shape enables the pouch motor to deform in a more controllable and

”linear” way. However, when fully inflated, the cross section of two perpendicular edges would become a tip and thus make the linear edges become distorted. For such reason, in this work, all pouch motors were designed in slot shapes. The arcs at both ends would help reducing unwanted deformation and maximize the desired output motions.

3.3.2 Air inlets and connectives

There are two design methods to integrate air nozzles in the fabrication of pneumatic soft pouch actuators. The first is to make inflate/deflate air channels directly with the design of pouches. After the main fabrication process, extra manual operations are needed to insert plastic nozzles into the soft, open channels.

The second method is to cut small air holes at desired locations on TPU films before the heat press step. After heat pressing, the air holes would not be affected and air nozzles could be made by directly 3d printing at the air holes’ locations. This method would create out-of-plane air inlets and should be combined with the mask heat pressing fabrication. Precise positioning is required, too.

With the air inlet nozzles, external soft tubes and air pressure sources could be connected to the fabricated soft actuators.

3.3.3 Equipment review

The 3d printer used in this work is Prusa[®] i3 MK3S+ with the corresponding slicer software ”PrusaSlicer”.

The heat press machine is ePhotoInc[®] Heat Press sized 16 X 24 inches.

The marker used in the mask heat pressing process is Quartet[®] dry eraser marker, black color.

Laser cutting machine: glowforge[™] Glowforge basic.

3.3.4 Recommended parameters for 3d printing

In this work, a 0.6mm extrusion hot nozzle is used on the 3d printer. According to the choice of filament materials, the optimal slicer settings to print extra structures on the heat pressed base layers may vary. Table 3.3 contains some of the recommended parameters for creating a solid bond between the 3d printed filament materials and the base layers while avoid over heating the base layer materials at the same time. These parameters are non-determined and should vary slightly on different 3d printers.

Table 3.3: Recommended 3d printing parameters for the monolithic fabrication. δ refers to the thickness of the heat pressed multi-layer base.

3d printing parameters	Filament materials		
	PLA	ABS	TPU Flex
Extruder temperature (°C)	210-220	250-260	230-240
Bed temperature (°C)	60-70	90-100	50-60
Layer height (mm)		0.15	
First layer height (mm)		0.2	
Z offset (mm)		[δ -0.5, δ -0.1]	
First Layer speed (mm/s)	4-6	5-10	5-8

3.4 Summary

In this section, the technique details of the proposed monolithic fabrication for pouch soft actuators have been explained. Two technique approaches, the filament welding method and the mask heat pressing method are developed. For the mask heat pressing process, the usage of plastic film mask and paint material mask have been explored, FEP plastic mask and alcohol based dry erase ink mask are found to

be the best known plastic and ink/paint material. With different layer arrangements of the heat pressing process, it is possible to create pouch actuated mechanisms with different configuration and properties, which proved the flexibility and potential in soft robotic application of the proposed fabrication.

Peel force tests were completed to help characterizing the heat pressing process; Preferred 3d printing parameters obtained from try and trial tests are given for future reference.

Chapter 4

Prototyping and Tests

In this chapter, some prototypes and corresponding tests will be presented to validate the proposed monolithic fabrication methods for soft robots.

4.1 Single Pouch Actuator Tests

To evaluate both the motion and force capabilities of the pouch actuators fabricated by the monolithic fabrications, block force and bending angle experiments of single pouch motors were designed and conducted.

4.1.1 Experiment setup

4 single pouch actuator test samples with different geometries were fabricated by the monolithic filament welding method. Fig.4.1 demonstrates the design and fabrication details of the pouch motor samples for this test. The 4 pouch motors have the shape of slots, their widths refer to the distances between two parallel sides, and their lengths are the offsets between the centers of the two semicircles.

The test platform composites of a load cell force sensor, an absolute gas pressure sensor. An LED screen is used to display the readings. The pressurized air was pro-

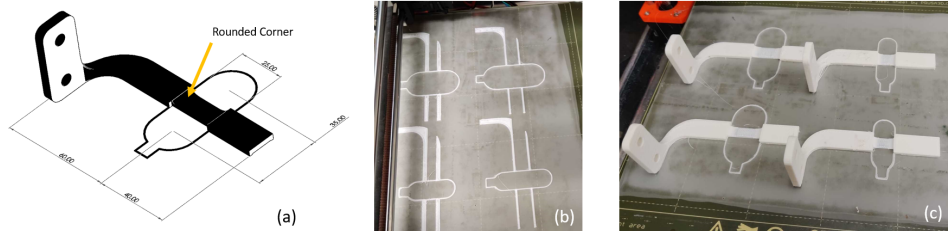


Figure 4.1: (a):Important dimensions of a pouch motor test sample. Each test sample has different length and width sizes while other dimensions stay unchanged. In this figure, the width $h = 25mm$ and the length $l = 35mm$; (b):Pouch motors sealed by 3d printer nozzles in the first layer and paused so that the support PC layers could be attached into the structures; (c):Complete pouch motor test samples made by the monolithic filament welding fabrication. Pouch sizes($h \times l$) are 15×25 , 15×35 , 25×25 , 25×35 , respectively in millimeters.

vided through a miniature pump and a flow restrictor valve connects the pneumatic system with the atmosphere. See Fig.4.2 for a real picture of the test platform and Fig.4.3 for the electric diagram.

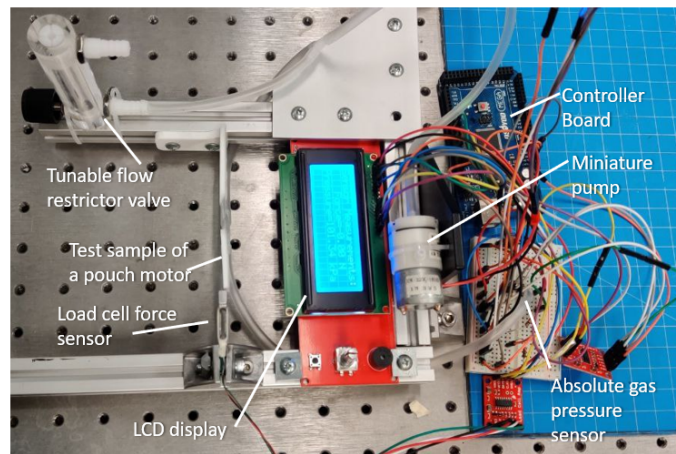


Figure 4.2: The test platform used for the bending angle and block force measurements.

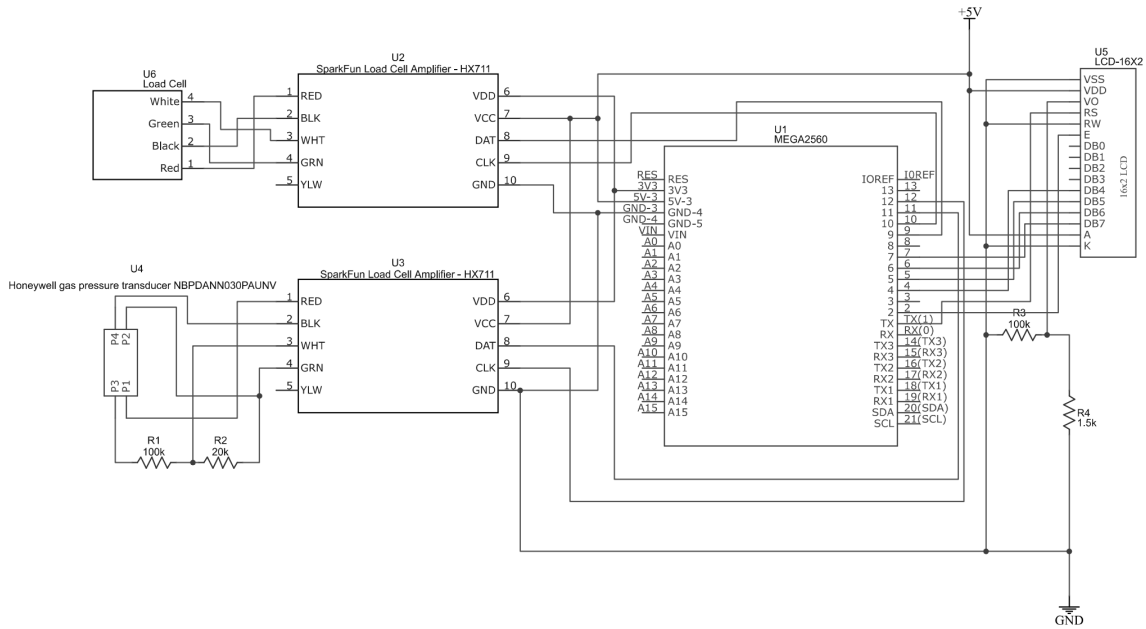


Figure 4.3: Electrical schematic of the test platform.

4.1.2 Measurements and results

For testing, simply connect the pouch motor into the pneumatic system, secure the sample to the frame at the right location, and turn on the miniature pump to pressurize the system. The pressure could be regulated by both tuning the flow restrictor valve and the voltage on the pump, mainly the latter approach.

Then, the free displacement (angles under zero force load) bending angles and block force (Output force with a zero bending angle) measurements of the four test samples could be obtained by taking pictures at any desired stabilized state, see Fig.4.4 for an example of the measurements.

Repeat measurements for each pouch motor samples under a sequence of different pressure values, the results are summarized in Fig.4.5. From the figures, it is known

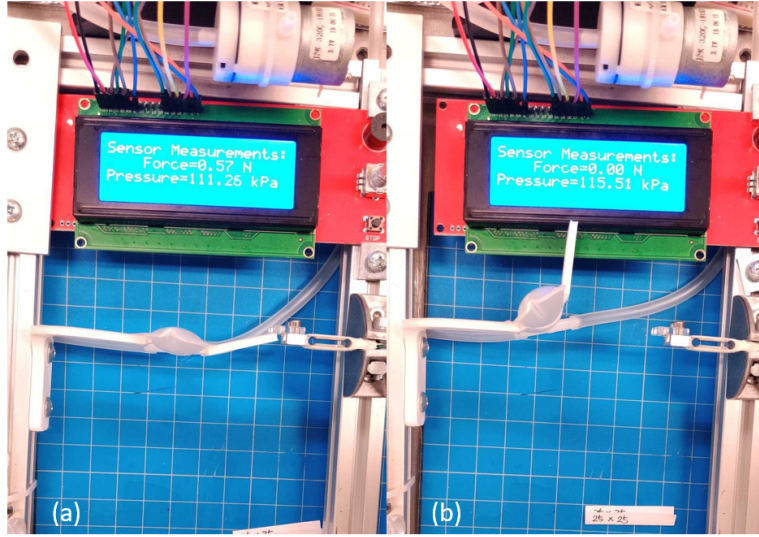


Figure 4.4: Examples of block force measurement(a) and bending angle measurement(b) of the pouch motor test sample with size $25\text{mm} \times 25\text{mm}$.

that the pouch motors made by the proposed fabrication method, given proper actuation pressure and geometry designs, could produce a significant motion as well as force output, thus could be used in soft robot applications.

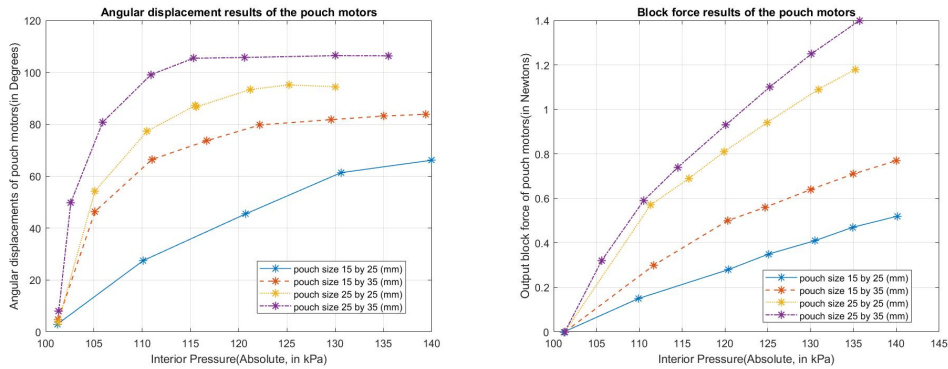


Figure 4.5: Bending angle and block force test results of the 4 pouch motor samples with different geometries.

4.2 Crawling robot demonstration

4.2.1 Crawling robot design and fabrication

Two sets of pouch actuators are located on the soft robot body one after another. The main body of the crawling robot is composed by 3d printed ABS material, and the pouch actuators were made by the filament welding process as discussed in chapter 3. A PC support layer was applied over the pouches so that they would bend downward when actuated. The main body of the robot has a length of 208mm, width 70mm and height 6mm. This size does not count the extra actuation units that need to be attached to the robot body. Fig.4.6 elaborates the monolithic fabrication process of the main robot body, which is quite similar to what's in Fig.3.4 in chapter 3.

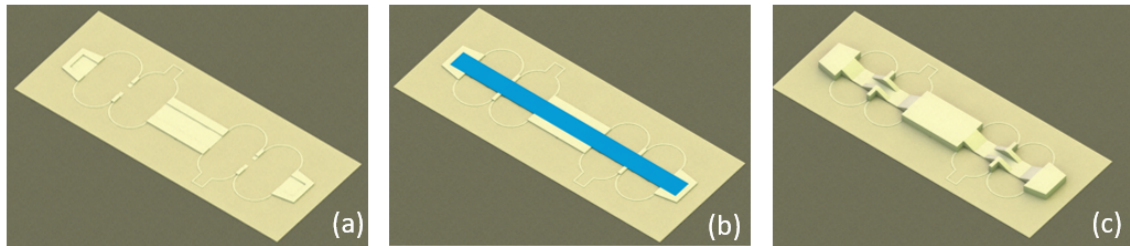


Figure 4.6: Schematic of the filament welding fabrication of the crawling robot. (a): 3d print the first layer, thermal weld the pouch actuators and bond the 3d printed material with heat pressed TPU base. (b): Pause right after finishing the first layer and attach the support layer over the pouches with adhesive. (c): Resume printing and finish top part of the model.

4.2.2 Pneumatic control and driving system

To generate a directional moving tendency of the robot body, it is needed to actuate the front and hind actuators in sequence. Here, an inchworm-like motion

sequence is used to move the soft robot. Two miniature solenoid valves are used to control two sets of actuators separately, a miniature pump provides pressured air to the robot, and a micro controller board is used to control the valves and pump. (See Fig.4.7)

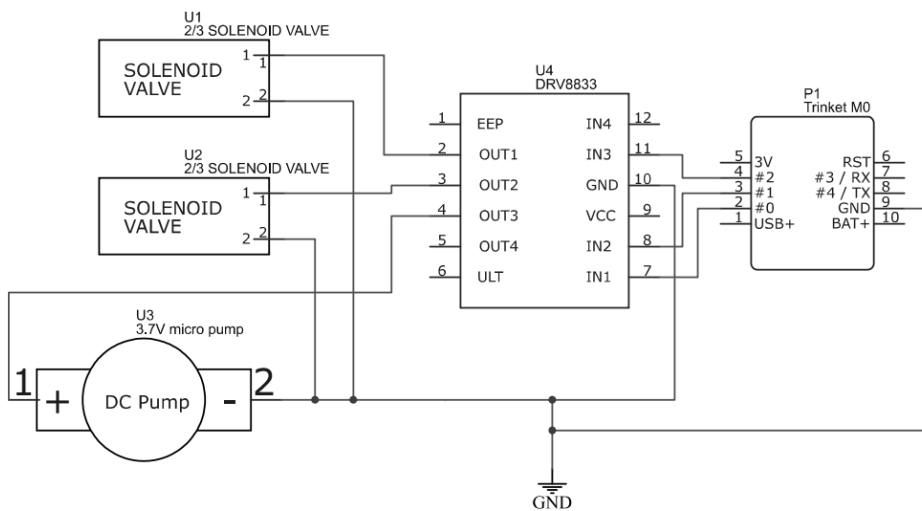


Figure 4.7: Electrical schematic of the crawling robot control system.

4.2.3 Movement demonstration

The motion capability of the crawling robot was tested by its movement on a flat wood surface. In Fig.4.9, the crawling robot is able to support its own weight and move forward under actuation with an approximate speed over 1cm/s ; Fig.4.8 demonstrates the actuation order of the pouch motors from a side view of the robot being hung on a test rack.

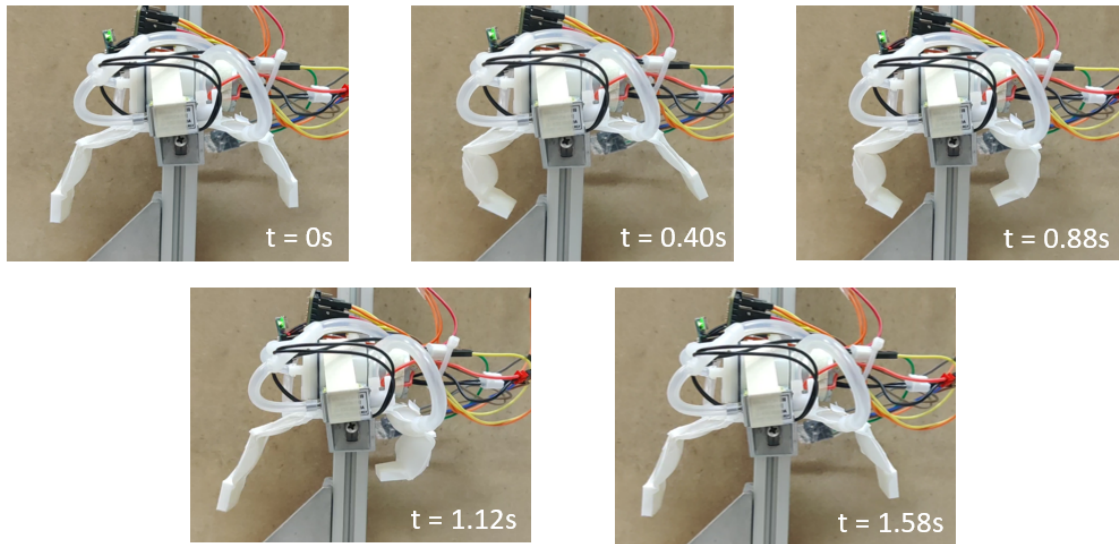


Figure 4.8: Motion sequence of the crawling robot. (hung in the air)

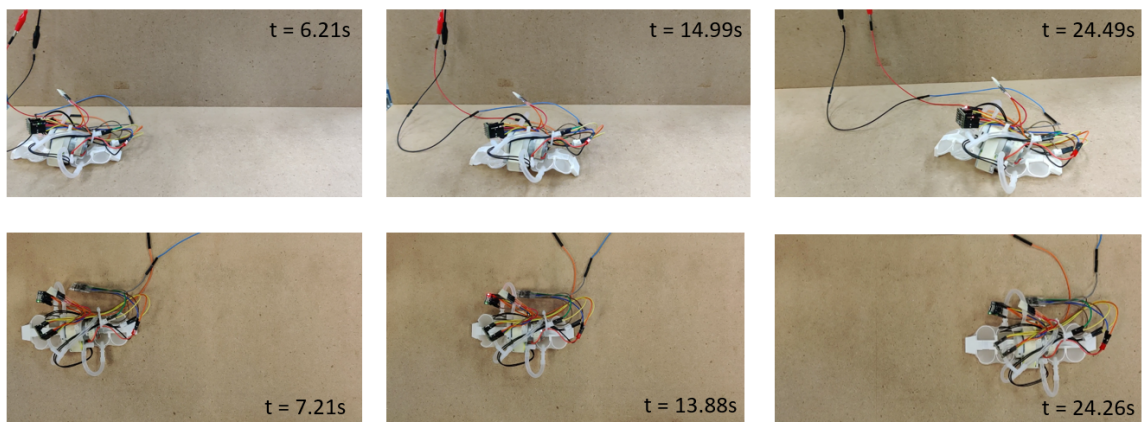


Figure 4.9: Motion sequence of the crawling robot moving on a wood surface. Top row: Side view of the crawling robot movement; Bottom row: Top view of the crawling robot movement.

4.3 Inherent motion sequence demonstration

4.3.1 Viscous flow control theory for soft robots

When passing through narrow gaps or channels, the effect of fluid (gas or liquid) viscosity would become significant, and time delays in fluid pressure or flow will emerge. This phenomenon could help to simplify the control systems of fluid soft robots, since the some kind of motion sequence control can be integrated within the actuators. A recent work[80] by Vasios, Nikolaos et al. explored on this concept extensively and in-depth. They tested an FEA soft robot system with narrow tubes to exploit the effects of viscous flow. In this part, the proposed monolithic fabrication method in this work will be utilized to make a soft actuator mechanism with inherent time sequence control.

4.3.2 Fabrication of a sequential soft actuator

The key to viscous flow control is the narrow channels. To fabricate usable narrow channels, the mask heat pressing fabrication should be used with FEP mask material, because even a small amount of thermal bond would prevent the narrow channels from opening under pressure actuation, FEP film is the only material known by now that doesn't heat-bond with TPU at all.

In this part, a bi-actuation soft mechanism was fabricated. Two FEP inserts were cut into the the shape of serial pouches and narrow channel ($2mm$ width) connections in between. Fig.4.10 demonstrates the heat pressed multi-layer base details and the finished structure. Notice that in this design the air connectors were made and bond with the base layer by direct 3d printing. The rigid top parts are 3d printed using ABS material, they support the whole structure and keep the deformation in regulated directions.

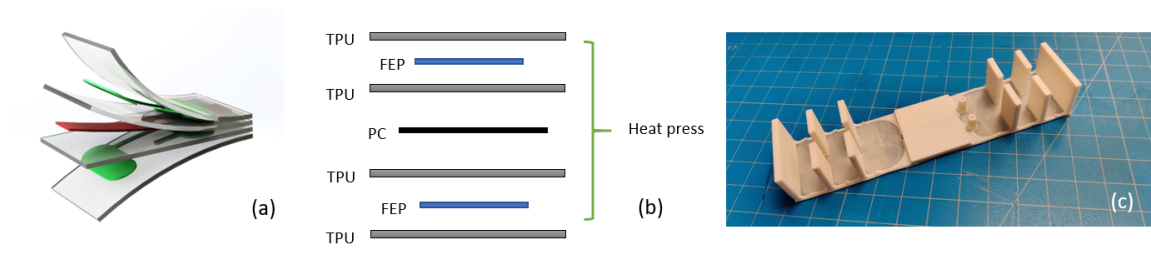


Figure 4.10: Schematic of the fabrication of a self-sequence actuator. (a),(b): The mask heat pressed multi-layer base with bi-directional setting. (c): The finished self-sequence soft actuator.

4.3.3 Motion demonstration

The fabricated actuator was connected to two syringes, each controls the actuation in one direction. By pressurizing the syringes alternatively, a cycling motion sequence is generated in the actuator. See Fig. for a recorded motion sequence with time stamps.

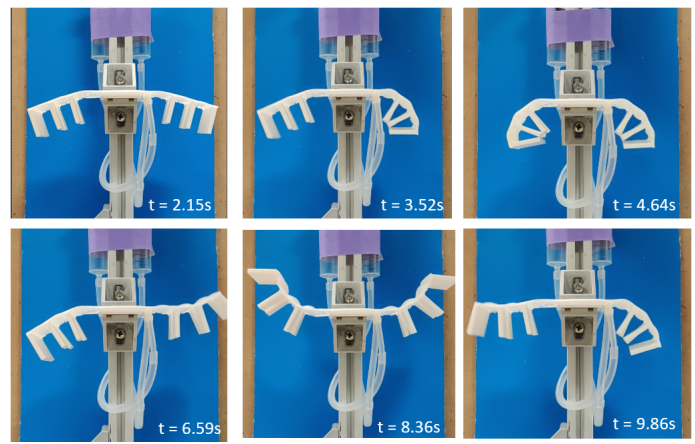


Figure 4.11: Motion sequence of the self-sequence actuator. The time delay between actuation on the left and right ends is created by the narrow, pneumatic viscous flow channels.

4.4 Summary

In this section, the proposed monolithic fabrication methods are tested and validated by prototyping of a crawling soft robot as well as an actuation mechanism with inherent, self-controlled time delay. With the variety of filament welding or mask heat pressing monolithic fabrication methods, and the flexibility of the arrangement of the heat pressed layers, these fabrications can suit different design and prototyping requirements.

Chapter 5

Conclusion and Future Works

5.1 Conclusion

In this work, a new family of monolithic fabrication methods for making low profile soft robot powered by pneumatic pouch actuators are proposed and developed. Combining the concepts of laminating, additive manufacturing, thermal bonding and pneumatic pouch motor actuating, the proposed fabrication methods are fast, cheap and flexible. Among the various sheet and film materials, TPU is found to be an excellent choice for pouch fabrication due to its thermal-bonding property with common FDM 3d printing filament materials such as PLA and ABS; PC is found to be a good material for support layers for similar reasons and its high rigidity and stiffness.

filament welding fabrications and mask heat pressing fabrications are two branches of the monolithic soft robot fabrication methods. The filament welding fabrication methods use the heat from 3d printer extruders to melt and seal the outlines of pouch motors, while the mask heat pressing methods use a mask between heat pressed TPU films to create inflatable chambers. The choice of mask material is tricky, the mask material could be some plastic film material or some ink or paint material which does

not bond with TPU under heat pressing. FEP and alcohol-carbon based marker ink are found to be the best film and ink mask material by so far, but there could be better choices which are still yet to be discovered. By arranging the order of heat pressed layers: mask layers, TPU layers and PC support layers in different ways, it is possible to create quite different multi-layer base of the structure and thus achieve different design objectives. Once the base layer is ready from heat pressing, it is then attached to the heat bed of a 3d printer and go through the final 3d printing process. With suitable choice of filament material and setting of parameters, a solid, strong bond will be created between the multi-layer base and the 3d printed structures. The 3d printing process would endow the structure with needed strength, rigidity and special geometry patterns at desired location. Positioning and alignment is crucial in this process.

A soft crawling robot and a bi-directional actuator with self-controlled motion sequence were fabricated through the proposed monolithic fabrication methods, their motion capabilities were also tested. The proposed monolithic fabrications were proved to have some extent of potential in soft robotics application.

5.2 Conceptual extension and future works

5.2.1 Embedded Sensors

This work has focused mostly on actuators. Embedded sensors, however, are very suitable to be integrated into this monolithic, lamination based fabrication process of low profile soft robot, too. In the future, a strain or bend sensor layer could be added to the multi-layer structure in this work to enable feed back controls.

5.2.2 Improved mask heat pressing process

The mask materials found in this work is far from optimal. Ideally, some paint or ink material with excellent non-stick property will be discovered in the future. This would help get rid of laser cutting steps in the process since the ink could be applied by a CNC drawing machine.

5.2.3 Possibility of valves and logic

Fluidic valves and logic gates have been widely used in micro-fluidic related research fields. By using the mask heat press method, it is also possible to create a multi-layer pneumatic system, where the flow resistance of a fluid channel is be controlled by a pouch in its adjacent layer. However, the feasibility of this research direction remains doubtful.

5.2.4 One-station fabrication center

If the monolithic fabrication methods in this work keeps being improved, some day there might be a highly integrated manufacturing center for the monolithic fabrication process. The film materials will be processed, masked and heat pressed automatically, a multi-material 3d printing system will then create sensitive, conductive or structural components on the base layer. This would allow massive production of small, low-cost soft robots.

Bibliography

- [1] D. Trivedi, C. D. Rahn, W. M. Kier, and I. D. Walker, “Soft robotics: Biological inspiration, state of the art, and future research,” *Applied Bionics and Biomechanics*, vol. 5, no. 3, p. 99–117, 2008.
- [2] D. Rus and M. T. Tolley, “Design, fabrication and control of soft robots,” *Nature*, vol. 521, no. 7553, p. 467–475, 2015.
- [3] K.-J. Cho, J.-S. Koh, S. Kim, W.-S. Chu, Y. Hong, and S.-H. Ahn, “Review of manufacturing processes for soft biomimetic robots,” *International Journal of Precision Engineering and Manufacturing*, vol. 10, no. 3, p. 171–181, 2009.
- [4] G.-K. Lau, G.-K. Lau, Y.-W. Chin, and K.-R. Heng, “Soft actuators and their fabrication for bio-inspired mobile robots,” *Proceedings of the 1st International Conference on Progress in Additive Manufacturing*, 2014.
- [5] F. Schmitt, O. Piccin, L. Barbé, and B. Bayle, “Soft robots manufacturing: A review,” *Frontiers in Robotics and AI*, vol. 5, 2018.
- [6] A. D. Marchese, R. K. Katzschmann, and D. Rus, “A recipe for soft fluidic elastomer robots,” *Soft Robotics*, vol. 2, no. 1, p. 7–25, 2015.
- [7] R. J. Wood, S. Avadhanula, R. Sahai, E. Steltz, and R. S. Fearing, “Microrobot design using fiber reinforced composites,” *Journal of Mechanical Design*, vol. 130, no. 5, 2008.
- [8] J. G. Cham, S. A. Bailey, J. E. Clark, R. J. Full, and M. R. Cutkosky, “Fast and robust: Hexapedal robots via shape deposition manufacturing,” *The International Journal of Robotics Research*, vol. 21, no. 10-11, p. 869–882, 2002.
- [9] H. Lipson and M. Kurman, *Fabricated: the new world of 3D printing*. John Wiley and Sons, 2013.

- [10] Y. Xia and G. M. Whitesides, “Soft lithography,” *Annual Review of Materials Science*, vol. 28, no. 1, p. 153–184, 1998.
- [11] C. D. Onal and D. Rus, “A modular approach to soft robots,” *2012 4th IEEE RAS & EMBS International Conference on Biomedical Robotics and Biomechanics (BioRob)*, 2012.
- [12] A. D. Marchese, C. D. Onal, and D. Rus, “Autonomous soft robotic fish capable of escape maneuvers using fluidic elastomer actuators,” *Soft Robotics*, vol. 1, no. 1, p. 75–87, 2014.
- [13] C. M. Schumacher, M. Loepfe, R. Fuhrer, R. N. Grass, and W. J. Stark, “3d printed lost-wax casted soft silicone monoblocks enable heart-inspired pumping by internal combustion,” *RSC Adv.*, vol. 4, no. 31, p. 16039–16042, 2014.
- [14] K. C. Galloway, K. P. Becker, B. Phillips, J. Kirby, S. Licht, D. Tchernov, R. J. Wood, and D. F. Gruber, “Soft robotic grippers for biological sampling on deep reefs,” *Soft Robotics*, vol. 3, no. 1, p. 23–33, 2016.
- [15] A. Argiolas, B. C. M. Murray, I. V. Meerbeek, J. Whitehead, E. Sinibaldi, B. Mazzolai, and R. F. Shepherd, “Sculpting soft machines,” *Soft Robotics*, vol. 3, no. 3, p. 101–108, 2016.
- [16] R. V. Martinez, J. L. Branch, C. R. Fish, L. Jin, R. F. Shepherd, R. M. D. Nunes, Z. Suo, and G. M. Whitesides, “Composite materials: Robotic tentacles with three-dimensional mobility based on flexible elastomers (adv. mater. 2/2013),” *Advanced Materials*, vol. 25, no. 2, p. 153–153, 2013.
- [17] H. Zhao, Y. Li, A. Elsamadisi, and R. Shepherd, “Scalable manufacturing of high force wearable soft actuators,” *Extreme Mechanics Letters*, vol. 3, p. 89–104, 2015.
- [18] L. Weiss, R. Merz, F. Prinz, G. Neplotnik, P. Padmanabhan, L. Schultz, and K. Ramaswami, “Shape deposition manufacturing of heterogeneous structures,” *Journal of Manufacturing Systems*, vol. 16, no. 4, p. 239–248, 1997.
- [19] X. Li, A. Golnas, and F. B. Prinz, “Shape deposition manufacturing of smart metallic structures with embedded sensors,” *Smart Structures and Materials 2000: Sensory Phenomena and Measurement Instrumentation for Smart Structures and Materials*, 2000.

- [20] M. Binnard and M. R. Cutkosky, “Design by composition for layered manufacturing,” *Journal of Mechanical Design*, vol. 122, no. 1, p. 91–101, 1999.
- [21] A. Dollar and R. Howe, “A robust compliant grasper via shape deposition manufacturing,” *IEEE/ASME Transactions on Mechatronics*, vol. 11, no. 2, p. 154–161, 2006.
- [22] T. G. Thuruthel, B. Shih, C. Laschi, and M. T. Tolley, “Soft robot perception using embedded soft sensors and recurrent neural networks,” *Science Robotics*, vol. 4, no. 26, 2019.
- [23] K. Elgeneidy, N. Lohse, and M. Jackson, “Bending angle prediction and control of soft pneumatic actuators with embedded flex sensors – a data-driven approach,” *Mechatronics*, vol. 50, p. 234–247, 2018.
- [24] B. Mosadegh, P. Polygerinos, C. Keplinger, S. W. Wennstedt, R. Shepherd, U. Gupta, J. Shim, K. Bertoldi, C. Walsh, and G. Whitesides, “Pneumatic networks for soft robotics that actuate rapidly,” *Advanced Functional Materials*, vol. 24, pp. 2163–2170, 2014.
- [25] Y. Sun, Y. S. Song, and J. Paik, “Characterization of silicone rubber based soft pneumatic actuators,” *2013 IEEE/RSJ International Conference on Intelligent Robots and Systems*, 2013.
- [26] J.-S. Koh and K.-J. Cho, “Omegabot : Biomimetic inchworm robot using sma coil actuator and smart composite microstructures (scm),” *2009 IEEE International Conference on Robotics and Biomimetics (ROBIO)*, 2009.
- [27] C. Sung and D. Rus, “Foldable joints for foldable robots,” *Experimental Robotics Springer Tracts in Advanced Robotics*, p. 421–433, 2015.
- [28] D. Haldane, C. Casarez, J. Karras, J. Lee, C. Li, A. Pullin, E. Schaler, D. Yun, H. Ota, A. Javey, and R. Fearing, “Integrated manufacture of exoskeletons and sensing structures for folded millirobots,” *Journal of Mechanisms and Robotics*, vol. 7, no. 2, 2015.
- [29] C. D. Onal, M. T. Tolley, R. J. Wood, and D. Rus, “Origami-inspired printed robots,” *IEEE/ASME Transactions on Mechatronics*, vol. 20, no. 5, p. 2214–2221, 2015.

- [30] H. D. Yang and A. T. Asbeck, “A new manufacturing process for soft robots and soft/rigid hybrid robots,” *2018 IEEE/RSJ International Conference on Intelligent Robots and Systems (IROS)*, 2018.
- [31] M. A. Robertson, O. C. Kara, and J. Paik, “Soft pneumatic actuator-driven origami-inspired modular robotic “pneumagami”,” *The International Journal of Robotics Research*, vol. 40, no. 1, pp. 72–85, 2021. [Online]. Available: <https://doi.org/10.1177/0278364920909905>
- [32] G. Stano and G. Percoco, “Additive manufacturing aimed to soft robots fabrication: A review,” *Extreme Mechanics Letters*, vol. 42, p. 101079, 2021.
- [33] R. V. Martinez, C. R. Fish, X. Chen, and G. M. Whitesides, “Elastomeric origami: Programmable paper-elastomer composites as pneumatic actuators,” *Advanced Functional Materials*, vol. 22, no. 7, p. 1376–1384, 2012.
- [34] Y. Zhang, N. Zhang, H. Hingorani, N. Ding, D. Wang, C. Yuan, B. Zhang, G. Gu, and Q. Ge, “Soft robots: Fast-response, stiffness-tunable soft actuator by hybrid multimaterial 3d printing (adv. funct. mater. 15/2019),” *Advanced Functional Materials*, vol. 29, no. 15, p. 1970098, 2019.
- [35] G. Stano, L. Arleo, and G. Percoco, “Additive manufacturing for soft robotics: Design and fabrication of airtight, monolithic bending pneunets with embedded air connectors,” *Micromachines*, vol. 11, no. 5, p. 485, 2020.
- [36] B. Keong and R. C.-H. Yeow, “A novel fold-based design approach toward printable soft robotics using flexible 3d printing materials,” *Advanced Materials Technologies*, vol. 3, 12 2017.
- [37] M. Jiang, Z. Zhou, and N. Gravish, “Flexoskeleton printing enables versatile fabrication of hybrid soft and rigid robots,” *Soft Robotics*, vol. 7, no. 6, p. 770–778, 2020.
- [38] J. Madden, N. Vandesteeg, P. Anquetil, P. Madden, A. Takshi, R. Pytel, S. Lafontaine, P. Wieringa, and I. Hunter, “Artificial muscle technology: physical principles and naval prospects,” *IEEE Journal of Oceanic Engineering*, vol. 29, no. 3, pp. 706–728, 2004.
- [39] K. Lee, N. Munce, T. Shoa, L. Charron, G. Wright, J. Madden, and V. Yang, “Fabrication and characterization of laser-micromachined polypyrrole-based artificial muscle actuated catheters,” *Sensors and Actuators A: Physical*, vol. 153, pp. 230–236, 05 2009.

- [40] C. Nguyen, N. Vuong, D. Kim, H. Moon, J. Koo, Y. Lee, J.-D. Nam, and H. Choi, “Fabrication and control of rectilinear artificial muscle actuator,” *Mechatronics, IEEE/ASME Transactions on*, vol. 16, pp. 167 – 176, 03 2011.
- [41] A. Nemiroski, Y. Shevchenko, A. Stokes, B. Ünal, A. Ainla, S. Albert, G. Compton, E. MacDonald, Y. Schwab, C. Zellhofer, and G. Whitesides, “ArthroBots,” *Soft Robotics*, vol. 4, no. 3, p. 183–190, 2017.
- [42] I. Walker and M. Hannan, “A novel ‘elephant’s trunk’ robot,” in *1999 IEEE/ASME International Conference on Advanced Intelligent Mechatronics (Cat. No.99TH8399)*, 1999, pp. 410–415.
- [43] L. Tang, J. Wang, Y. Zheng, G. Gu, L. Zhu, and X. Zhu, “Design of a cable-driven hyper-redundant robot with experimental validation,” *International Journal of Advanced Robotic Systems*, vol. 14, no. 5, p. 172988141773445, 2017.
- [44] M. Calisti, M. Giorelli, G. Levy, B. Mazzolai, B. Hochner, C. Laschi, and P. Dario, “An octopus-bioinspired solution to movement and manipulation for soft robots,” *Bioinspiration & Biomimetics*, vol. 6, no. 3, p. 036002, 2011.
- [45] T. Deng, H. Wang, W. Chen, X. Wang, and R. Pfeifer, “Development of a new cable-driven soft robot for cardiac ablation,” *2013 IEEE International Conference on Robotics and Biomimetics (ROBIO)*, 2013.
- [46] F. Renda, M. Giorelli, M. Calisti, M. Cianchetti, and C. Laschi, “Dynamic model of a multibending soft robot arm driven by cables,” *IEEE Transactions on Robotics*, vol. 30, no. 5, p. 1109–1122, 2014.
- [47] D. Zappetti, R. Arandes, E. Ajanic, and D. Floreano, “Variable-stiffness tensegrity spine,” *Smart Materials and Structures*, vol. 29, no. 7, p. 075013, 2020.
- [48] M. Cianchetti, “Fundamentals on the use of shape memory alloys in soft robotics,” *Interdisciplinary Mechatronics*, p. 227–254, 2013.
- [49] M. Behl, K. Kratz, J. Zotzmann, U. Nöchel, and A. Lendlein, “Reversible bidirectional shape-memory polymers,” *Advanced Materials*, vol. 25, no. 32, p. 4466–4469, 2013.
- [50] J.-H. Youn, S. M. Jeong, G. Hwang, H. Kim, K. Hyeon, J. Park, and K.-U. Kyung, “Dielectric elastomer actuator for soft robotics applications and challenges,” *Applied Sciences*, vol. 10, no. 2, p. 640, 2020.

- [51] R. Lumia and M. Shahinpoor, “Ipmc microgripper research and development,” *Journal of Physics: Conference Series*, vol. 127, p. 012002, 2008.
- [52] J. Sohn, G.-W. Kim, and S.-B. Choi, “A state-of-the-art review on robots and medical devices using smart fluids and shape memory alloys,” *Applied Sciences*, vol. 8, no. 10, p. 1928, 2018.
- [53] Q. He, Z. Wang, Y. Wang, A. Minori, M. T. Tolley, and S. Cai, “Electrically controlled liquid crystal elastomer–based soft tubular actuator with multimodal actuation,” *Science Advances*, vol. 5, no. 10, 2019.
- [54] B. P. Lee, M.-H. Lin, A. Narkar, S. Konst, and R. Wilharm, “Modulating the movement of hydrogel actuator based on catechol–iron ion coordination chemistry,” *Sensors and Actuators B: Chemical*, vol. 206, p. 456–462, 2015.
- [55] B. P. Lee, A. Narkar, and R. Wilharm, “Effect of metal ion type on the movement of hydrogel actuator based on catechol-metal ion coordination chemistry,” *Sensors and Actuators B: Chemical*, vol. 227, p. 248–254, 2016.
- [56] M. Agerholm and A. Lord, “The ”artificial muscle” of mckibben,” *The Lancet*, vol. 277, no. 7178, p. 660–661, 1961.
- [57] C.-P. Chou and B. Hannaford, “Measurement and modeling of mckibben pneumatic artificial muscles,” *IEEE Transactions on Robotics and Automation*, vol. 12, no. 1, p. 90–102, 1996.
- [58] H. S. Cho, T. H. Kim, T. H. Hong, and Y.-L. Park, “Ratchet-integrated pneumatic actuator (ripa): a large-stroke soft linear actuator inspired by sarcomere muscle contraction,” *Bioinspiration & Biomimetics*, vol. 15, no. 3, p. 036011, 2020.
- [59] N. D. Naclerio and E. W. Hawkes, “Simple, low-hysteresis, foldable, fabric pneumatic artificial muscle,” *IEEE Robotics and Automation Letters*, vol. 5, no. 2, pp. 3406–3413, 2020.
- [60] J. Walker, T. Zidek, C. Harbel, S. Yoon, F. S. Strickland, S. Kumar, and M. Shin, “Soft robotics: A review of recent developments of pneumatic soft actuators,” *Actuators*, vol. 9, no. 1, p. 3, 2020.

- [61] P. Polygerinos, N. Correll, S. Morin, B. Mosadegh, C. Onal, K. Petersen, M. Cianchetti, M. Tolley, and R. Shepherd, “Soft robotics: Review of fluid-driven intrinsically soft devices; manufacturing, sensing, control, and applications in human-robot interaction: Review of fluid-driven intrinsically soft robots,” *Advanced Engineering Materials*, vol. 19, p. e201700016, 05 2017.
- [62] K. Suzumori, S. Iikura, and H. Tanaka, “Applying a flexible microactuator to robotic mechanisms,” *IEEE Control Systems Magazine*, vol. 12, no. 1, pp. 21–27, 1992.
- [63] R. Shepherd, F. Ilievski, W. Choi, S. Morin, A. Stokes, A. Mazzeo, X. Chen, M. Wang, and G. Whitesides, “Multigait soft robot,” *Proceedings of the National Academy of Sciences of the United States of America*, vol. 108, pp. 20 400–3, 11 2011.
- [64] M. T. Tolley, R. F. Shepherd, B. Mosadegh, K. C. Galloway, M. Wehner, M. Karpelson, R. J. Wood, and G. M. Whitesides, “A resilient, untethered soft robot,” *Soft Robotics*, vol. 1, no. 3, p. 213–223, 2014.
- [65] R. Katzschmann, A. Marchese, and D. Rus, “Hydraulic autonomous soft robotic fish for 3d swimming,” in *ISER*, vol. 109, 06 2014, pp. 405–420.
- [66] P. Polygerinos, Z. Wang, K. C. Galloway, R. Wood, and C. Walsh, “Soft robotic glove for combined assistance and at-home rehabilitation,” *Robotics Auton. Syst.*, vol. 73, pp. 135–143, 2015.
- [67] R. Niiyama, D. Rus, and S. Kim, “Pouch motors: Printable/inflatable soft actuators for robotics,” *2014 IEEE International Conference on Robotics and Automation (ICRA)*, 2014.
- [68] R. Niiyama, X. Sun, C. Sung, B. An, D. Rus, and S. Kim, “Pouch motors: Printable soft actuators integrated with computational design,” *Soft Robotics*, vol. 2, no. 2, p. 59–70, 2015.
- [69] X. Sun, S. M. Felton, R. Niiyama, R. J. Wood, and S. Kim, “Self-folding and self-actuating robots: A pneumatic approach,” *2015 IEEE International Conference on Robotics and Automation (ICRA)*, 2015.
- [70] J. Ou, M. Skouras, N. Vlavianos, F. Heibeck, C.-Y. Cheng, J. Peters, and H. Ishii, “Aeromorph - heat-sealing inflatable shape-change materials for interaction design,” in *Proceedings of the 29th Annual Symposium on User*

Interface Software and Technology, ser. UIST '16. New York, NY, USA: Association for Computing Machinery, 2016, p. 121–132. [Online]. Available: <https://doi.org/10.1145/2984511.2984520>

- [71] Q. Lu, J. Ou, J. Wilbert, A. Haben, H. Mi, and H. Ishii, “millimorph – fluid-driven thin film shape-change materials for interaction design,” *Proceedings of the 32nd Annual ACM Symposium on User Interface Software and Technology*, 2019.
- [72] M. Zhu, T. N. Do, E. Hawkes, and Y. Visell, “Fluidic fabric muscle sheets for wearable and soft robotics,” *Soft Robotics*, vol. 7, no. 2, p. 179–197, 2020.
- [73] A. A. A. Moghadam, S. Alaie, S. D. Nath, M. A. Shaarbaq, J. K. Min, S. Dunham, and B. Mosadegh, “Laser cutting as a rapid method for fabricating thin soft pneumatic actuators and robots,” *Soft Robotics*, vol. 5, no. 4, p. 443–451, 2018.
- [74] A. A. A. Moghadam, A. Caprio, S. Alaie, J. K. Min, S. Dunham, and B. Mosadegh, “Rapid manufacturing of thin soft pneumatic actuators and robots,” *Journal of Visualized Experiments*, no. 153, 2019.
- [75] N. Kellaris, V. G. Venkata, G. M. Smith, S. K. Mitchell, and C. Keplinger, “Peano-hassel actuators: Muscle-mimetic, electrohydraulic transducers that linearly contract on activation,” *Science Robotics*, vol. 3, no. 14, 2018.
- [76] S. K. Mitchell, X. Wang, E. Acome, T. Martin, K. Ly, N. Kellaris, V. G. Venkata, and C. Keplinger, “An easy-to-implement toolkit to create versatile and high-performance hasel actuators for untethered soft robots,” *Advanced Science*, p. 1900178, 2019.
- [77] M. Fatahillah, N. Oh, and H. Rodrigue, “A novel soft bending actuator using combined positive and negative pressures,” *Frontiers in Bioengineering and Biotechnology*, vol. 8, 2020.
- [78] W. Kim, H. Park, and J. Kim, “Compact flat fabric pneumatic artificial muscle (ffpam) for soft wearable robotic devices,” *IEEE Robotics and Automation Letters*, vol. 6, no. 2, p. 2603–2610, 2021.
- [79] H. Lee, N. Oh, and H. Rodrigue, “Expanding pouch motor patterns for programmable soft bending actuation: Enabling soft robotic system adaptations,” *IEEE Robotics & Automation Magazine*, vol. 27, no. 4, p. 65–74, 2020.

- [80] N. Vasios, A. J. Gross, S. Soifer, J. T. Overvelde, and K. Bertoldi, “Harnessing viscous flow to simplify the actuation of fluidic soft robots,” *Soft Robotics*, vol. 7, no. 1, p. 1–9, 2020.